AALBORG UNIVERSITY

DENMARK

Wind Loads on Dynamic Sensitive Structures

Mørk, K. J.; Kirkegaard, Poul Henning; Sørensen, John Dalsgaard

[Link to publication from Aalborg University](#)

Wind Loads on Dynamic Sensitive Structures

K.J. Mørk, P.H. Kirkegaard & J.D. Sørensen

Wind Loads on Dynamic Sensitive Structures

K.J. Mørk†, P.H. Kirkegaard‡ & J.D. Sørensen‡

†Det Norske Veritas,Offshore Classification and Technical Services
Veritasveien 1, N-1322 Høvik

‡Aalborg University, Department of Building Technology and Structural Engineering
Sohngaardsholmsvej 57, DK-9000 Aalborg

Preface

This note has been prepared for the course on "Loads on Offshore Structures" given on the 9th semester of the M.Sc. study programme on Structural Engineering at Aalborg University.

The object of the note is to give a generally applicable description of wind load as well as the response of a structure sensitive to wind load. The description is limited to address load due to mean wind, transverse fluctuations, vortex shedding and motion induced load. Therefore, aeroelastic phenomena as galloping and flutter are not included. The gust factor method based on stochastic oscillation analysis has been applied as a design tool.

The note assumes fundamental knowledge of the deterministic and stochastic vibration theory for continuous structures. Further, a certain knowledge of hydrodynamics and safety and reliability theory is required.

Aalborg University, March 1992.

Kim Mørk

In agreement with Kim Mørk we have translated the note from Danish to English and updated it in accordance with the new Danish Code, *Code of Practice for Loads for the Design of Structures* (DS410). Further, the note has been extended with a numerical example.

Aalborg University, November 1999.

Poul Henning Kirkegaard & John Dalsgaard Sørensen

Contents

List of Figures

List of Tables

Chapter 1

Along-wind load

1.1 Introduction

The along-wind load per unit area q on a structure is normally proportional with the velocity pressure.

$$q = \frac{1}{2}\rho v^2 \tag{1.1}$$

where $\rho = 1.25$ kg/m^3 is the air density and v is the wind velocity. The along-wind load per unit area is then found by multiplying q by a shape factor C_D.

The natural wind field may be assumed to be composed of a mean wind velocity and turbulence of stochastic nature. Due to the turbulence the wind velocity and thus the wind load vary with time. In principle the wind load shall therefore be considered a dynamic and stochastic load.

If the load is varying slowly in relation to the lowest natural frequency of the structure, the damping and inertia loads of the structure will be negligible compared to being considered a static load. This will normally be the case for conventional building structures. If, on the other hand, the natural frequencies of the structure are relatively low, as e.g. in tall, slender buildings, the dynamic load of the wind is significant.

In accordance with DS 410 [1], the dynamic effects of the wind shall be taken into consideration for structures assumed to vibrate due to wind turbulence.

In the present note a general description of the wind load and the along-wind response of a vibration dynamic sensitive structure is addressed. Further, across-wind vibration due to vortex shedding is mentioned and an analysis procedure taking account of the across-wind vibration due to the movements of the structure, the so-called *lock-in* phenomenon, is given. In [2] more details concerning wind loads on structures can be found.

1.2 Natural wind

For the description of the natural wind field the following assumptions are applied:

- At a sufficient height above terrain, where the conditions are independent of friction at the ground surface, the flow is assumed to be horizontally homogeneous (geostrophic wind).

- The terrain is horizontal.

- The terrain roughness is constant.

- The stability is neutral, i.e. the thermal contribution to the turbulence is disregarded (permissible for wind velocities above 10 m/s, [2]).

- The wind field is considered a weakly stationary process (10 min. observation intervals).

- No change of wind direction with the height above terrain. (Measurements show that the wind direction is only changed by a few degrees up to a height of 180 m, [3]).

The above assumptions imply that a horizontally homogeneous boundary layer flow is assumed.

A coordinate system is introduced with the x-axis in the wind direction, the y-axis perpendicular to the wind direction, designated the across-wind direction, and the z-axis vertically upwards. The wind velocities $U_x(x, y, z, t)$, $U_y(x, y, z, t)$ and $U_z(x, y, z, t)$ at a given time can be expressed as

$$U_x(x, y, z, t) = v(z) + u_x(x, y, z, t) \tag{1.2}$$

$$U_y(x, y, z, t) = 0 + u_y(x, y, z, t) \tag{1.3}$$

$$U_z(x, y, z, t) = 0 + u_z(x, y, z, t) \tag{1.4}$$

where $v(z)$ is the mean wind velocity and $u_x(x, y, z, t)$, $u_y(x, y, z, t)$ and $u_z(x, y, z, t)$ are the turbulence of the wind field considered as weakly stationary stochastic processes with mean value 0. In figure 1.1 an instantaneous picture of the along-wind variation of the wind field with the height z is shown.

1.3 Wind profiles

An analysis of dimensions shows that the mean velocity of the boundary layer flow may be expressed by the logarithmic profile

z, height

$U_x(x, y, z, t)$

$v(z)$
Mean wind velocity

$u_x(x, y, z, t)$
Turbulence component
in the wind direction

x
Wind direction

y
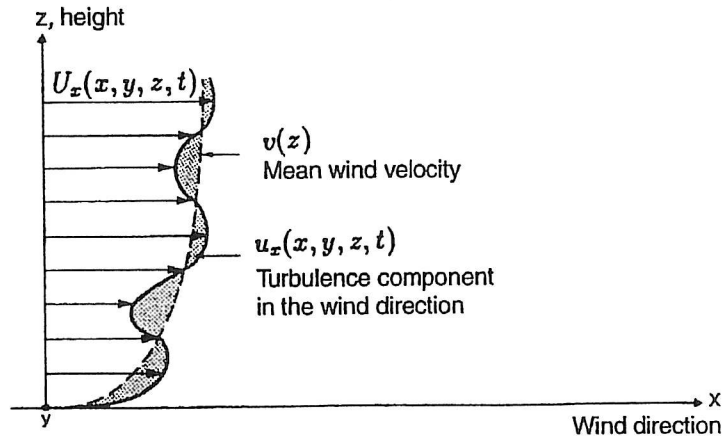
Figure 1.1: *Instantaneous picture of the along-wind variation of the wind field with the height z.*

$$v(z) = v_* \frac{1}{\kappa} \ln \frac{z}{z_0} \quad (z < 200 \text{ m}) \tag{1.5}$$

where v_* : the rate of friction (friction velocity) in the boundary layer.
κ : von Karman's constant ≈ 0.408.
z_0 : roughness parameter $(z_0 \in [10^{-5}, 10]m)$.

The mean wind velocity corresponding to the 50 year return period wind is normally expressed as

$$v_m(z) = v_b k_t \ln \frac{z}{z_0} \tag{1.6}$$

where v_b : basic wind velocity.
k_t : terrain parameter.

For a 50 year wind the probability of a mean wind velocity larger than $v_m(z)$ during one year is 0.02, i.e. a 2 % exceedence probability.

v_b corresponding to the 10 min. mean wind velocity at 10 m height is denoted the basic wind velocity and is a 50 year wind. The basic wind velocity for Denmark are specified as 24-27 m/s for Denmark in [1] with the highest value for structures close to the west-coast. In [1] v_b is also multiplied by a topograpic factor, a direction factor and a seasonal factor.

Using (1.5) and (1.6) the friction velocity v_* may be described by

$$v_* = \kappa \cdot k_t \cdot v_b \tag{1.7}$$

1.4 Gust wind loading

The along-wind load per unit height w at the height z and at the time t for a one-dimensional structure with height h and diameter d sensitive to vibration can be written

$$w(z,t) = \frac{1}{2}\rho \left(v(z) + u_x(z,t) - \dot{x}(z,t)\right)^2 d(z)C_D(z) \tag{1.8}$$

where
$$
\begin{array}{lll}
v(z) & : & \text{mean wind velocity.} \\
u_x(z,t) & : & \text{along-wind turbulence.} \\
\dot{x}(z,t) & : & \text{velocity of the structure.} \\
d(z) & : & \text{width of wind exposed structural member.} \\
C_D(z) & : & \text{shape factor.} \\
\rho & : & \text{air density.}
\end{array}
$$

The term $(v(z) + u_x(z,t) - \dot{x}(z,t))$ is denoted the relative velocity. Empirically, $v(z) \gg u_x(z,t)$ and $v(z) \gg \dot{x}(z,t)$, whereby

$$\left(v(z) + u_x(z,t) - \dot{x}(z,t)\right)^2 \approx v(z)^2 + 2v(z)u_x(z,t) - 2v(z)\dot{x}(z,t) \tag{1.9}$$

Thus, the wind load can be divided into the following contributions

$$w(z,t) = w_s(z) + w_t(z,t) - w_a(z,t) \tag{1.10}$$

where
$$
\begin{array}{llll}
w_s(z) & = & \frac{1}{2}g(z)v(z) & : \text{quasi-static load due to } v(z). \\
w_t(z,t) & = & g(z)u_x(z,t) & : \text{load due to wind turbulence.} \\
w_a(z,t) & = & g(z)\dot{x}(z,t) & : \text{aerodynamic damping due to } \dot{x}(z,t). \\
g(z) & = & \rho v(z)d(z)C_D(z) & : \text{transition function.}
\end{array}
$$

1.5 Load due to wind turbulence

1.5.1 General definitions

In wind analysis the cross-spectrum $S_{XY}(\omega)$ is defined for the processes $\{X(t), Y(t), t \in T\}$ by the following version of the Wiener-Khintchine relations, [2]

$$S_{XY}(\omega) = 2 \int_{-\infty}^{\infty} \kappa_{XY}(\tau)e^{-i\omega\tau}\, d\tau \tag{1.11}$$

$$\kappa_{XY}(\tau) = \frac{1}{4\pi} \int_{-\infty}^{\infty} S_{XY}(\omega)e^{i\omega\tau}\, d\omega \tag{1.12}$$

The variance of the process $\{X(t), t \in T\}$ is found from (1.12)

$$\sigma_X^2 = \frac{1}{2\pi} \int_0^\infty S_{XX}(\omega) \, d\omega \qquad (1.13)$$

The cross-spectrum $S_{XY}(\omega)$ is generally complex. On the other hand, the auto-spectrum $S_{XX}(\omega)$, where only positive cyclic frequencies ω are applied corresponding to a one-sided spectrum, is always real. The cross-spectrum can be written as

$$S_{XY}(\omega) = |S_{XY}(\omega)| e^{i\Phi_{XY}(\omega)} \qquad (1.14)$$

where $|S_{XY}(\omega)|$ and $\Phi_{XY}(\omega)$ are designated the cross-amplitude spectrum and the phase spectrum, respectively. For wind technical analysis a coherence spectrum is often used, which is defined as

$$Coh_{XY}(\omega) = \frac{|S_{XY}(\omega)|^2}{S_{XX}(\omega) S_{YY}(\omega)} \qquad (1.15)$$

The coherence is a measure of the statistical dependence of the processes $\{X(t), \ t \in T\}$ and $\{Y(t), \ t \in T\}$, cf. the analogy for the correlation coefficient between two stochastic variables.

Based on (1.14) and (1.15) the cross-spectrum may be written

$$S_{XY}(\omega) = \sqrt{S_{XX}(\omega)} \sqrt{S_{YY}(\omega)} \sqrt{Coh_{XY}(\omega)} e^{i\Phi_{XY}(\omega)} \qquad (1.16)$$

1.5.2 Load contribution due to wind turbulence

Due to wind turbulence the load can be written as, cf. (1.10)

$$w_t(z, t) = g(z) u_x(z, t), \quad g(z) = \rho v(z) d(z) C_D(z) \qquad (1.17)$$

The turbulence load can be written on spectral form by considering the cross-covariance function $\kappa_{w_t w_t}(z_1, z_2, \tau)$ for the turbulent wind load at the heights z_1 and z_2, where τ is the time interval $(t_2 - t_1)$

$$\kappa_{w_t w_t}(z_1, z_2, \tau) = E[(w_t(z_1, t_1) - \mu_{w_t}(z_1, t_1))(w_t(z_2, t_2) - \mu_{w_t}(z_2, t_2))] \qquad (1.18)$$

$$\mu_{u_x} = 0 \Rightarrow \mu_{w_t} = 0 \Rightarrow$$

$$\kappa_{w_t w_t}(z_1, z_2, \tau) = E[g(z_1)u_x(z_1, t_1)g(z_2)u_x(z_2, t_2)]$$
$$= g(z_1)g(z_2)\kappa_{u_x u_x}(z_1, z_2, \tau) \tag{1.19}$$

Applying the Wiener-Khintchine relation (1.11) on both sides of the equation sign,

$$S_{w_t w_t}(z_1, z_2, \omega) = g(z_1)g(z_2)S_{u_x u_x}(z_1, z_2, \omega) \tag{1.20}$$

It is known that the imaginary part of the cross-spectral densities of the load process do not have any influence on the auto-spectral density of the response process. Applying (1.16) it is found that the real part of the cross-spectrum $S_{w_t w_t}(z_1, z_2, \omega)$ for the turbulence load can be written as

$$S_{w_t w_t}(z_1, z_2, \omega) = g(z_1)g(z_2)\sqrt{S_{u_x}(z_1, \omega)S_{u_x}(z_2, \omega)}\sqrt{Coh_{u_x u_x}(z_1, z_2, \omega)} \cdot$$
$$\cos(\Phi_{u_x u_x}(z_1, z_2, \omega)) \tag{1.21}$$

Note that if the points z_1 and z_2 coincide, the auto-spectrum $S_{w_t}(z, \omega)$ is obtained from (1.21) for the turbulent wind load. Now, only a description of the auto-spectrum $S_{u_x}(z, \omega)$ for the turbulent wind load component, the coherens-spectrum $Coh_{u_x u_x}(z_1, z_2, \omega)$ and the phase-spectrum $\Phi_{u_x u_x}(z_1, z_2, \omega)$ remains.

1.5.3   Auto-spectra

Since the response of the structure and along wind load are considered, only along-wind turbulence is addressed at first. The energy distribution of the turbulence on the different frequencies is described by an auto-spectrum. From an analysis of dimensions, [8], it is established that the auto-spectrum is given on the form

$$S_{u_x}(z, \omega) = \alpha \frac{v_*^2}{\frac{\omega}{2\pi}} \frac{\left(\frac{\omega}{2\pi}\frac{L_u(z)}{v(10)}\right)^\beta}{\left[\gamma + \left(\frac{\omega}{2\pi}\frac{L_u(z)}{v(10)}\right)^\epsilon\right]^\delta} \tag{1.22}$$

where $L_u(z)$ is a length scale describing the magnitude of the turbulence vortices. The parameters α, β, δ, ϵ and γ are assumed to have different values belonging to the four most frequently used spectra, given by Davenport, [6], Harris, [3], Simiu, [7] and DS410, [1,2], respectively. The values of the parameters are given in table 1.1. It should be noticed that DS410, [1], gives the non-dimensional auto-spectrum $R_N(z, \omega) = \frac{\omega}{2\pi}\frac{S_{u_x}(\omega)}{\sigma_{u_x}^2}$.

It is seen from the table that the spectra proposed by Davenport and Harris are independent of height, while Simiu's spectrum and the spectrum in DS 410 are dependent on the

	α	β	γ	ϵ	δ	$L_u(z)$	$\sigma^2_{u_x}/v^2_*$
Davenport	4	2	1	2	$\frac{4}{3}$	1200 m	6
Harris	4	1	2	2	$\frac{5}{6}$	1800 m	6.65
Simiu	4	1	1	1	$\frac{5}{3}$	$50\frac{v(10)}{v(z)}z$ m	6
DS 410	0.851	1	0.098	1	$\frac{5}{3}$	$\begin{cases} L(z_{min}) & z < z_{min} \\ 100(\frac{z}{10})^{0.3}\frac{v(10)}{v(z)} & z \geq z_{min} \end{cases}$	6

Table 1.1: *Turbulence spectra for velocity fluctuations $u_x(z)$.*

height z above terrain. From the boundary layer theory it is known that the magnitude of the vortices grow beyond the boundary layer, causing the length scale expressing the mean of the turbulent turbulent vortices, to increase with the height. This is not taken into account in the two spectra that are independent of height. In [4] it is shown that the difference between the response obtained from different spectra becomes large for increasing height of the structure.

In the right hand column in table 1.1 the variance $\sigma^2_{u_x}$ is defined by (1.13) calculated as

$$\sigma^2_{u_x}(z) = \frac{1}{2\pi} \int_0^\infty S_{u_x}(z,\omega) \, d\omega \tag{1.23}$$

It is noted that all 4 spectra have approximately the same energy characterised by the variance $\sigma^2_{u_x}$ normalized with regard to the friction velocity v_*.

The above-mentioned four spectra $S_{u_x}(z,\omega)$ as a function of ω are shown as a double-logarithmic curve in figure 1.2. The friction velocity v_* is determined corresponding to the terrain class $z_0=0.05$.

It is seen from the figure that particularly Simiu's spectrum contains most energy from the background turbulence ($\omega \ll 1$). Further, it is seen that the turbulence energy distribution in the DS410 spectrum is distributed over a relatively wide frequency band. If the energy distribution is described by the Davenport spectrum it is expected to give the largest dynamic load contribution resonant with the first eigen-frequency of the structure ω_1 when $\omega_1 > 0.1$. On the other hand it can be mentioned that the along-wind dynamic response for tall, lightly damped structures will be considerably reduced if Simiu's auto-spectrum is applied instead of one of the others, [8]. The simple spectral form (1.22) gives an accurate representation of the turbulent fluctuations in the frequency range of interest for most structures. However, for structures with a very low fundamental frequency, e.g. offshore structures, a more accurate auto-spectrum should be used. In [5] the following Højstrup auto-spectrum is proposed for the low-frequency part of the spectrum

$$S_{u_x}(z,\omega) = \frac{v_*^2}{\frac{\omega}{2\pi}} \left(\frac{5n\frac{A_l}{z}}{1 + 2.2\left(n\frac{A_l}{z}\right)^{5/3}} + \frac{105n}{(1+33n)^{5/3}} \right) \frac{1}{1 + 7.4\left(\frac{z}{A_l}\right)^{2/3}} \qquad (1.24)$$

where $n = \frac{\omega z}{2\pi v(z)}$ and a neutral length scale $A_l = 3000$ m. (1.24) holds well for measurements at 10 m and above. For lower levels [5] gives an expression for the length scale A_l as a function of z. From figure 1.2 it is seen that the energy from the background turbulence will be underestimated by using the auto-spectra given in table 1.1.
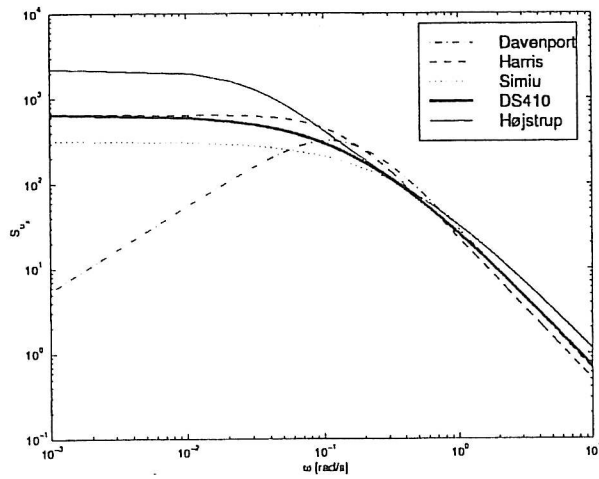
(a) Turbulence spectrum at the height z=10 m
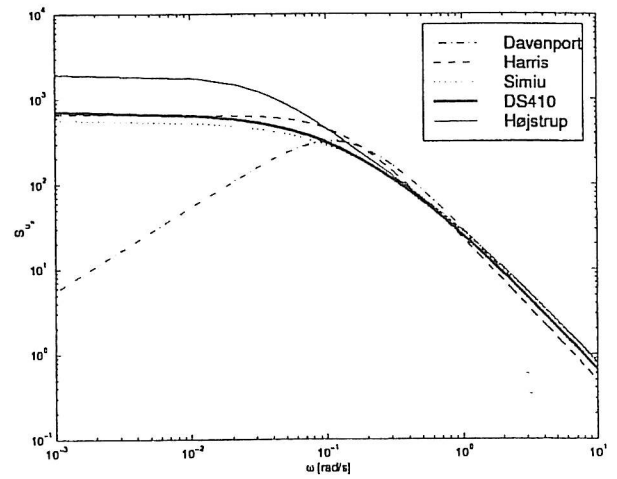
(b) Turbulence spectrum at the height z=20 m
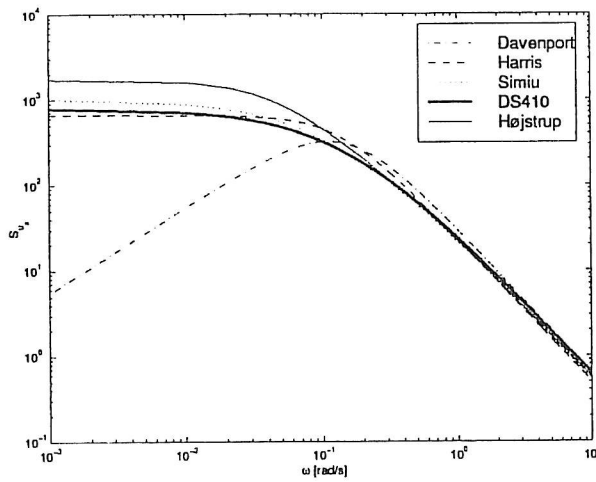
(c) Turbulence spectrum at the height z=40 m
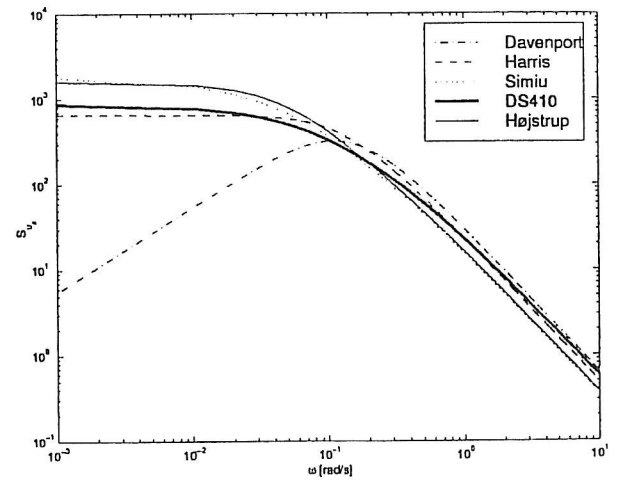
(d) Turbulence spectrum at the height z=80 m

Figure 1.2: *Turbulence spectra shown for different heights.*

1.5.4   The coherence spectrum

As mentioned, the coherence spectrum describes the statistical dependence between the turbulence at two points at a given cyclic frequency. This dependence due to the limited spatial extension of the vortices of the wind field will have to decrease with the distance $|z_1 - z_2|$ between the two points z_1 and z_2. This decay depends on the magnitude of the vortex which can be measured by $v(\bar{z})T$, where $v(\bar{z}) = \frac{1}{2}(v(z_1) + v(z_2))$ and $T = 2\pi/\omega$ is the period of the vortices with the cyclic frequency ω.

Using a plan perpendicular to the wind direction, Davenport [6] and Shiotani & Iwatani, [10] have proved by experimental full-scale tests that the vertical coherence spectrum can be expressed as

$$Coh_{u_x u_x}(z_1, z_2, \omega) = \exp\left(-2C\frac{\omega}{2\pi}\frac{|z_1 - z_2|}{v(\bar{z})}\right) \tag{1.25}$$

where C is a non-dimensional decay constant dependent on the height. Full-scale tests, [6,8,10] have shown that C decreases with the height and is moderately dependent on the terrain roughness and the mean wind velocity. Measurements at Stigsnæs [8] shows that $C \sim 10$ for points located 10-20 m vertically above one another. It is noted that (1.25) may be subject to some gross uncertainty at large distances $|z_1 - z_2|$ and small cyclic frequencies.

1.5.5   The phase spectrum

Based on the above-mentioned full-scale tests, the phase spectrum $\Phi_{u_x u_x}(z_1, z_2, \omega)$ described in [10] is estimated to

$$\Phi_{u_x u_x}(z_1, z_2, \omega) = k\frac{\omega}{2\pi}\frac{(z_1 - z_2)}{v(\bar{z})} \tag{1.26}$$

where k is a non-dimensional constant. Empirically, $k \approx 7 - 8$, [8].

1.6   Aerodynamic damping

The load contribution to the wind load from the movement of the structure (1.10) due to aerodynamic damping is introduced by adding the aerodynamic damping ratio ζ_m^a corresponding to the m'th mode shape to the structural damping of the building ζ_m^s, i.e.

$$\zeta_m = \zeta_m^s + \zeta_m^a \tag{1.27}$$

The contribution from the aerodynamic damping force $w_a(t)$ can be written as

$$w_a(z,t) = g(z)\dot{x}(z,t) = \rho v(z)d(z)C_D(z)\dot{x}(z,t) = c_a(z)\dot{x}(z,t) \tag{1.28}$$

On assumption of fulfillment of the decoupling requirement (1.29)

$$\int_0^h \Phi_m(z)c_a(z)\Phi_n(z)dz = \begin{cases} 0 & ,m \neq n \\ 2\zeta_m^a M_m\omega_m & ,m = n \end{cases} \tag{1.29}$$

where Φ_m : m'th fundamental mode in bending in the in x-direction.
        ω_m : m'th cyclic eigen-frequency.
        M_m :   modal mass of the m'th mode shape (defined by (3.4), see chapter 3).

the along-wind aerodynamic damping of the m'th eigen mode can be determined as

$$\zeta_m^a = \frac{1}{2M_m\omega_m} \int_0^h \rho v(z)d(z)C_D(z)\Phi_m^2(z)dz \tag{1.30}$$

The aerodynamic damping causes an increased dissipation of mechanical energy and thus a reduction of the vibration level of the structure.

Chapter 2

Gust factor method

Since the wind loading and the structural response are considered as stochastic processes a statistical analysis has to be used in a design situation. As a design tool we will use the expected maximum $E[X_{max}]$ of the maximal value process $\{X_{\max}(t),\ t \in T\}$ belonging to the response process $\{X(t),\ t \in T\}$

$$E[X_{\max}] = \begin{cases} \varphi_X \mu_X & \mu_X \neq 0 \\ k_p \sigma_X & \mu_X = 0 \end{cases} \tag{2.1}$$

where φ_X is the *gust factor* and k_p is the *peak factor*. The gust factor is defined as the factor which multiplied by the expected value μ_X of the process $\{X(t),\ t \in T\}$ gives the expected values of the maximal value process

$$\varphi_X = \frac{E[X_{\max}]}{\mu_X} = 1 + k_p \frac{\sigma_X}{\mu_X} \tag{2.2}$$

where k_p : peak factor.

σ_X: standard deviation of X.

μ_X: expected value of X.

For a given reference time interval T the peak factor k_p of a narrow-banded Gaussian process is given by [11]

$$k_p = \sqrt{2\ln[\frac{1}{2\pi}\frac{\sigma_{\dot{X}}}{\sigma_X}T]} + \frac{\gamma}{\sqrt{2\ln[\frac{1}{2\pi}\frac{\sigma_{\dot{X}}}{\sigma_X}T]}} \tag{2.3}$$

where γ : Eulers constant = 0.5772.

$\sigma_{\dot{X}}$: standard deviation of $\dot{X}$.

T : time interval .

If the response process is not narrow-banded k_p is given by other expressions [2,16].

Chapter 3

Dynamic response of structures due to along-wind load

This section will outline how the wind load and dynamic response can be obtained for 1- and 2 dimensional structures based on a stochastic response analysis. Further, the relationship between the stochastic response analysis and the rules in DS 410, [1], for dynamic wind load estimation is explained. At last an example is given which presents results obtained from a stochastic response analysis and the rules in DS410 for a steel chimney, respectively.

3.1 Basic equations for 1-dimensional models

It is assumed that the structure can be modeled by a 1-dimensional model. The height of the model is assumed to be h.

3.1.1 Variance functions σ_X^2 and $\sigma_{\dot{X}}^2$ for response

The response process $\{X(t), t \in T\}$ is modeled by a modal expansion

$$X(z,t) = \sum_{m=1}^{\infty} q_m(t)\Psi_m(z) \tag{3.1}$$

where

$$\Psi_m(z) = \begin{cases} \Phi_m(z) & \text{for the displacement process } x(z,t). \\ \dfrac{d}{dz}\Phi_m(z) & \text{for the rotation process } \alpha(z,t). \\ EI(z)\dfrac{d^2\Phi_m(z)}{dz^2} & \text{for the bending moment process } M(z,t). \end{cases} \tag{3.2}$$

where q_m :   is the m'th modal coordinate.

       $\Phi_m(z)$:   is the m'th mode shape.

       z :   is the height.

       t :   is the time.

The mth modal coordinate function $q_m(t)$ is obtained as the solution to the differential equation

$$\ddot{q}_m(t) + 2\zeta_m\omega_m\dot{q}_m(t) + \omega_m^2 q_m(t) = \frac{1}{M_m}P_m(t) \tag{3.3}$$

where ω_m is the cyclical eigen-frequency for the mth vibration mode and M_m is the modal mass for the mth vibration mode. M_m is determined from the orthogonality condition

$$\int_0^h \Phi_m(z)\mu(z)\Phi_n(z)dz = \begin{cases} 0 & , \quad m \neq n \\ M_m & , \quad m = n \end{cases} \tag{3.4}$$

where h is the height of the structure and $\mu(z)$ is the mass per unit height. $P_m(t)$ is the modal load defined by

$$P_m(t) = \int_0^h \Phi_m(z)w_t(z,t)dz \tag{3.5}$$

where $w_t(z,t)$ is the wind load.

If the assumptions that the modal coordinates decouple and that the load has lasted for very long time are fulfilled then the solution to the differential equation (3.3) is given by the Duhamel integral

$$q_m(t) = \int_{-\infty}^t h_m(t-\tau)P_m(\tau)d\tau \tag{3.6}$$

where the impulse response function is given by

$$h_m(t) = \begin{cases} 0 & , t \leq 0 \\ \dfrac{1}{M_m\omega_{m,d}}\exp(-\zeta_m\omega_m t)\sin(\omega_{m,d}t) & , t > 0 \end{cases} \tag{3.7}$$

$\omega_{m,d}$ is the damped cyclical eigen-frequency

$$\omega_{m,d} = \omega_m\sqrt{1-\zeta_m^2} \tag{3.8}$$

The auto-spectral density function $S_{XX}(z,\omega)$ for the response $X(t)$ is determined from

$$S_{XX}(z,\omega) = \sum_{m=1}^\infty \sum_{n=1}^\infty \Psi_m(z)\Psi_n(z)S_{q_m q_n}(\omega) \tag{3.9}$$

where $S_{q_m q_n}(\omega)$ is the cross-spectral density for the modal coordinate process. Using (3.6) $S_{q_m q_n}(\omega)$ can be obtained from

$$S_{q_m q_n}(\omega) = H_m^*(\omega) H_n(\omega) S_{P_m P_n}(\omega) \tag{3.10}$$

where

$$H_m(\omega) = \frac{1}{(\omega_m^2 - \omega^2 + 2\zeta_m \omega_m \omega i) M_m} = \frac{1}{\omega_m^2 M_m} \frac{1}{\left(1 - \left(\dfrac{\omega}{\omega_m}\right)^2 + 2\zeta_m \dfrac{\omega}{\omega_m} i\right)} \tag{3.11}$$

is the modal frequency response function (* indicates complex conjugate) and $S_{P_m P_n}(\omega)$ is the cross-spectral density function for the modal load which is determined using (3.5)

$$S_{P_m P_n}(\omega) = \int_0^h \int_0^h \Phi_m(z_1) \Phi_n(z_2) S_{w_t w_t}(z_1, z_2, \omega) dz_1 dz_2 \tag{3.12}$$

$S_{w_t w_t}(z_1, z_2, \omega)$ is the cross-spectral density function for the wind load.

The variances of the response $X(t)$ and of the derivative of the response $\dot{X}(t)$ can then be calculated from

$$\sigma_X^2(z) = \frac{1}{2\pi} \sum_{m=1}^{\infty} \sum_{n=1}^{\infty} \Psi_m(z) \Psi_n(z) \int_0^{\infty} H_m^*(\omega) H_n(\omega) S_{P_m P_n}(\omega) d\omega \tag{3.13}$$

$$\sigma_{\dot{X}}^2(z) = \frac{1}{2\pi} \sum_{m=1}^{\infty} \sum_{n=1}^{\infty} \Psi_m(z) \Psi_n(z) \int_0^{\infty} \omega^2 H_m^*(\omega) H_n(\omega) S_{P_m P_n}(\omega) d\omega \tag{3.14}$$

If it also can be assumed that only the N lowest modes contribute significantly to the response the double summations in (3.13) and (3.14) can be simplified to

$$\sum_{m=1}^{\infty} \sum_{n=1}^{\infty} \rightsquigarrow \sum_{m=1}^{N} \sum_{n=1}^{N} \tag{3.15}$$

Further, if it can be assumed that the eigen-frequencies are well separated then the cross-terms in (3.13) and (3.14) can be neglected and the variances are determined from

$$\sigma_X^2(z) \approx \frac{1}{2\pi} \sum_{m=1}^{\infty} \Psi_m^2(z) \int_0^{\infty} |H_m(\omega)|^2 S_{P_m P_m}(\omega) d\omega \tag{3.16}$$

$$\sigma_{\dot{X}}^2(z) \approx \frac{1}{2\pi} \sum_{m=1}^{\infty} \Psi_m^2(z) \int_0^{\infty} \omega^2 |H_m(\omega)|^2 S_{P_m P_m}(\omega) d\omega \tag{3.17}$$

Further, if it can be assumed that the structure is lightly damped and that the load is broad-banded then (3.16) and (3.17) can be simplified to

$$\sigma_X^2(z) \approx \frac{1}{8} \sum_{m=1}^{N} \Psi_m^2(z) \frac{S_{P_m P_m}(\omega_m)}{\zeta_m \omega_m^3 M_m^2} \tag{3.18}$$

$$\sigma_{\dot{X}}^2(z) \approx \frac{1}{8} \sum_{m=1}^{N} \Psi_m^2(z) \frac{S_{P_m P_m}(\omega_m)}{\zeta_m \omega_m M_m^2} \tag{3.19}$$

By the white-noise approximation (3.18) and (3.19) the background turbulence contribution to the response is neglected. But a significant computational simplification is obtained.

3.1.2 Expected value function μ_X for response

The expected value of the response process $X(t)$ can be determined as the statically response of the structure with the statically wind load as load

$$\mu_X(z) \approx \sum_{m=1}^{N} \mu_{q_m}(z) \Psi_m(z) \tag{3.20}$$

Since the load is statically ($\dot{q}_m \approx \ddot{q}_m \approx 0$) it is seen from (3.3) and (3.5) that

$$\omega_m^2 \mu_{q_m} = \frac{1}{M_m} \int_0^h \Phi_m(s) w_s(s) ds \tag{3.21}$$

where $w_s(z)$ is the statically wind load. Thus

$$\mu_X(z) \approx \sum_{m=1}^{N} \Psi_m(s) \frac{1}{\omega_m^2 \, M_m} \int_0^h \Phi_m(s) w_s(s) ds \tag{3.22}$$

Alternatively, $\mu_X(z)$ can be obtained from

$$\mu_X(z) = \int_0^h w_s(s) X_I(z, s) ds \tag{3.23}$$

where $X_I(z, s)$ is the influence function for the response in height z given a unit load in height s.

3.1.3 Approximations for $N=1$ mode shape

If the response can be estimated with sufficient accuracy using only one mode shape, i.e. $N=1$ then the variance σ_X^2 can be determined from

$$
\begin{aligned}
\sigma_X^2(z) &= \frac{1}{2\pi}\Psi_1^2(z)\int_0^\infty |H_1(\omega)|^2 S_{P_1P_1}(\omega)d\omega \\
&= \frac{1}{2\pi}\Psi_1^2(z)\int_0^\infty |H_1(\omega)|^2 \int_0^h\int_0^h \Phi_1(z_1)\Phi_1(z_2)g(z_1)g(z_2)S_{u_xu_x}(z_1,z_2,\omega)dz_1dz_2d\omega \\
&\approx \frac{1}{2\pi}\Psi_1^2(z)|H_1(0)|^2 \int_0^\infty\int_0^h\int_0^h \Phi_1(z_1)\Phi_1(z_2)g(z_1)g(z_2)S_{u_xu_x}(z_1,z_2,\omega)dz_1dz_2d\omega + \\
&\quad \frac{1}{2\pi}\Psi_1^2(z)\int_0^\infty |H_1(\omega)|^2 d\omega \int_0^h\int_0^h \Phi_1(z_1)\Phi_1(z_2)g(z_1)g(z_2)S_{u_xu_x}(z_1,z_2,\omega_1)dz_1dz_2 \\
&= \frac{1}{2\pi}\Psi_1^2(z)\frac{1}{(\omega_1^2M_1)^2}\sigma_u^2\int_0^\infty\int_0^h\int_0^h \Phi_1(z_1)\Phi_1(z_2)g(z_1)g(z_2)\frac{S_{u_xu_x}(z_1,z_2,\omega)}{\sigma_u^2}dz_1dz_2d\omega + \\
&\quad \frac{1}{2\pi}\Psi_1^2(z)\frac{2\pi}{8\zeta_1\omega_1^3M_1^2}\int_0^h\int_0^h \Phi_1(z_1)\Phi_1(z_2)g(z_1)g(z_2)S_{u_xu_x}(z_1,z_2,\omega_1)dz_1dz_2 \\
&\approx (\mu_X(z)2I_u(z_{ref}))^2(k_b+k_r)
\end{aligned}
\tag{3.24}
$$

where the turbulence intensity I_u is defined by

$$
I_u = \frac{\sigma_u(z)}{v(z)}
\tag{3.25}
$$

The background factor k_b and the resonance factor k_r are given by

$$
\begin{aligned}
k_b &= \frac{1}{2\pi}\frac{1}{\left(\int_0^h \Phi_1(z)g(z)dz\right)^2}\int_0^\infty\int_0^h\int_0^h \Phi_1(z_1)\Phi_1(z_2)g(z_1)g(z_2)\frac{S_{u_xu_x}(z_1,z_2,\omega)}{\sigma_u^2}dz_1dz_2d\omega \\
&\approx \frac{1}{1+1.5\dfrac{h}{L(z_{ref})}}
\end{aligned}
\tag{3.26}
$$

$$
\begin{aligned}
k_r &= \frac{1}{8}\frac{\omega_1}{\zeta_1}\frac{1}{\left(\int_0^h \Phi_1(z)g(z)dz\right)^2}\int_0^h\int_0^h \Phi_1(z_1)\Phi_1(z_2)g(z_1)g(z_2)\frac{S_{u_xu_x}(z_1,z_2,\omega_1)}{\sigma_u^2}dz_1dz_2 \\
&\approx \frac{1}{2}\frac{\pi^2}{\delta_s+\delta_a}\frac{n_1S_{u_x}(z_{ref},n_1)}{\sigma_u^2}K_s(n_1)
\end{aligned}
\tag{3.27}
$$

where $n_1 = \dfrac{\omega_1}{2\pi}$: is the lowest natural (eigen-) frequency.

$\delta_s = 2\pi\zeta_{1s}$: is the structural damping coefficient for lowest eigen-frequency.

$\delta_a = 2\pi\zeta_{1a}$: is the aerodynamic damping coefficient for lowest eigen-frequency.

$K_s(n_1)$: is the size reduction factor given by,

$$K_s(n_1) = \frac{\displaystyle\int_0^h \int_0^h \Phi_1(z_1)\Phi_1(z_2)g(z_1)g(z_2)\sqrt{Coh_{u_x u_x}(z_1, z_2, n_1)}\,dz_1 dz_2}{\left(\displaystyle\int_0^h \Phi_1(z)g(z)dz\right)^2} \tag{3.28}$$

The approximations for k_b and k_r are used in DS410 and they are obtained based on a reference height z_{ref}, see section 3.3. Further, the phase spectrum is on the safe side neglected.

The variance $\sigma_{\dot{X}}^2$ can similarly be determined by from

$$
\begin{aligned}
\sigma_{\dot{X}}^2(z) &= \frac{1}{2\pi}\Psi_1^2(z)\int_0^\infty \omega^2|H_1(\omega)|^2 S_{P_1 P_1}(\omega)d\omega \\
&= \frac{1}{2\pi}\Psi_1^2(z)\int_0^\infty \omega^2|H_1(\omega)|^2 \int_0^h\int_0^h \Phi_1(z_1)\Phi_1(z_2)g(z_1)g(z_2)S_{u_x u_x}(z_1, z_2, \omega)dz_1 dz_2 d\omega \\
&\approx \frac{1}{2\pi}\Psi_1^2(z)|H_1(0)|^2\int_0^\infty\int_0^h\int_0^h \omega^2\Phi_1(z_1)\Phi_1(z_2)g(z_1)g(z_2)S_{u_x u_x}(z_1, z_2, \omega)dz_1 dz_2 d\omega + \\
&\quad \frac{1}{2\pi}\Psi_1^2(z)\int_0^\infty \omega^2|H_1(\omega)|^2 d\omega \int_0^h\int_0^h \Phi_1(z_1)\Phi_1(z_2)g(z_1)g(z_2)S_{u_x u_x}(z_1, z_2, \omega_1)dz_1 dz_2 \\
&= \frac{1}{2\pi}\Psi_1^2(z)\frac{1}{(\omega_1^2 M_1)^2}\sigma_u^2\int_0^\infty\int_0^h\int_0^h \omega^2\Phi_1(z_1)\Phi_1(z_2)g(z_1)g(z_2)\frac{S_{u_x u_x}(z_1, z_2, \omega)}{\sigma_u^2}dz_1 dz_2 d\omega + \\
&\quad \frac{1}{2\pi}\Psi_1^2(z)\frac{2\pi}{8\zeta_1\omega_1 M_1^2}\int_0^h\int_0^h \Phi_1(z_1)\Phi_1(z_2)g(z_1)g(z_2)S_{u_x u_x}(z_1, z_2, \omega_1)dz_1 dz_2 \\
&\approx (\mu_X(z)2I_u(z_{ref}))^2(k_b + k_r) \tag{3.29}
\end{aligned}
$$

where the factors k_b and k_r are given by

$$k_b = \frac{1}{2\pi}\frac{1}{\left(\displaystyle\int_0^h \Phi_1(z)g(z)dz\right)^2}\int_0^\infty\int_0^h\int_0^h \omega^2\Phi_1(z_1)\Phi_1(z_2)g(z_1)g(z_2)\frac{S_{u_x u_x}(z_1, z_2, \omega)}{\sigma_u^2}dz_1 dz_2 d\omega \tag{3.30}$$

$$k_r = \frac{1}{8}\frac{\omega_1^3}{\zeta_1}\frac{1}{\left(\displaystyle\int_0^h \Phi_1(z)g(z)dz\right)^2}\int_0^h\int_0^h \Phi_1(z_1)\Phi_1(z_2)g(z_1)g(z_2)\frac{S_{u_x u_x}(z_1, z_2, \omega_1)}{\sigma_u^2}dz_1 dz_2 \tag{3.31}$$

3.1.4 Approximations for N mode shapes

If N modes shapes are considered σ_X^2 can be determined from

$$
\begin{aligned}
\sigma_X^2(z) &= \frac{1}{2\pi} \sum_{m=1}^{N} \sum_{n=1}^{N} \Psi_m(z)\Psi_n(z) \int_0^\infty H_m^*(\omega)H_n(\omega) \cdot \\
&\qquad \int_0^h \int_0^h \Phi_m(z_1)\Phi_n(z_2)g(z_1)g(z_2)S_{u_x u_x}(z_1, z_2, \omega)dz_1 dz_2 d\omega \\
&\approx \frac{1}{2\pi} \sum_{m=1}^{N} \Psi_m^2(z)|H_m(0)|^2 \int_0^\infty \int_0^h \int_0^h \Phi_m(z_1)\Phi_n(z_2)g(z_1)g(z_2)S_{u_x u_x}(z_1, z_2, \omega)dz_1 dz_2 d\omega \\
&\qquad \frac{1}{2\pi} \sum_{m=1}^{N} \Psi_m^2(z) \int_0^\infty |H_m(\omega)|^2 d\omega \int_0^h \int_0^h \Phi_1(z_1)\Phi_1(z_2)g(z_1)g(z_2)S_{u_x u_x}(z_1, z_2, \omega_m)dz_1 dz_2 \\
&\approx (\mu_X(z)2I_u(z_{ref}))^2 (k_b + k_{r_1} + ... + k_{r_N})
\end{aligned}
\tag{3.32}
$$

where the background factor k_b and the resonance factor k_{r_m} are given by

$$
k_b = \frac{1}{2\pi} \frac{1}{\left(\displaystyle\sum_{m=1}^{N} \int_0^h \Phi_m(z)g(z)dz\right)^2} \sum_{m=1}^{N} \int_0^\infty \int_0^h \int_0^h \Phi_m(z_1)\Phi_m(z_2)g(z_1)g(z_2)\frac{S_{u_x u_x}(z_1, z_2, \omega)}{\sigma_u^2}dz_1 dz
\tag{3.33}
$$

$$
k_{r_m} = \frac{1}{8}\frac{\omega_m}{\zeta_m} \frac{1}{\left(\displaystyle\sum_{m=1}^{N} \int_0^h \Phi_m(z)g(z)dz\right)^2} \int_0^h \int_0^h \Phi_m(z_1)\Phi_m(z_2)g(z_1)g(z_2)\frac{S_{u_x u_x}(z_1, z_2, \omega_m)}{\sigma_u^2}dz_1 dz_2
\tag{3.34}
$$

The variance $\sigma_{\dot{X}}^2$ can be determined similarly.

3.1.5 Equivalent quasi-static wind load

Equivalent quasi-static wind load can be defined by

$$
w_e(z) = (1 + 2k_p I_u(z))\sqrt{k_b + k_{r_1} + ... + k_{r_N}}\, w_s(z)
\tag{3.35}
$$

where the static load $w_s(z)$ is defined by (1.10).

3.2 Basic equations for 2-dimensional models

Now, it is assumed that the structure can be modeled by a 2-dimensional model in the (y, z)-coordinate system where the z-coordinate is the height and the y-coordinate is the width. The dimensions of the model are assumed to be h and d .

3.2.1 Variance functions σ_X^2 and $\sigma_{\dot{X}}^2$ for response

The response process $\{X(t), t \in T\}$ is modeled by a modal expansion

$$X(z, y, t) = \sum_{m=1}^{\infty} q_m(t) \Phi_m(y, z) \tag{3.36}$$

where q_m :   is the m'th modal coordinate.
        $\Phi_m(y, z)$:   is the m'th mode shape.
        z :   is the height.
        y :   is the width.

The modal coordinate function $q_m(t)$ is obtained as the solution to the differential equation

$$\ddot{q}_m(t) + 2\zeta_m \omega_m \dot{q}_m(t) + \omega_m^2 q_m(t) = \frac{1}{M_m} P_m(t) \tag{3.37}$$

where ω_m is the cyclical eigen-frequency for the mth vibration mode and M_m is the modal mass for the mth vibration mode. M_m is determined from the orthogonality condition

$$\int_0^h \int_0^d \Phi_m(y, z) \mu(y, z) \Phi_n(y, z) dy dz = \begin{cases} 0 & , & m \neq n \\ M_m & , & m = n \end{cases} \tag{3.38}$$

$\mu(y, z)$ is the mass per unit area. $P_m(t)$ is the modal load defined by

$$P_m(t) = \int_0^h \int_0^d \Phi_m(y, z) w_t(y, z, t) dz dy \tag{3.39}$$

where $w_t(y, z, t)$ is the wind load.

The auto-spectral density function $S_{XX}(y, z, \omega)$ for the response $X(t)$ in coordinate (y, z) is determined from

$$S_{XX}(y, z, \omega) = \sum_{m=1}^{\infty} \sum_{n=1}^{\infty} \Phi_m(y, z) \Phi_n(y, z) S_{q_m q_n}(\omega) \tag{3.40}$$

where $S_{q_m q_n}(\omega)$ is the cross-spectral density for the modal coordinate process. The cross-spectral density function for the modal load is determined using (3.39)

$$S_{P_m P_n}(\omega) = \int_0^h \int_0^h \int_0^d \int_0^d \Phi_m(y_1, z_1) \Phi_n(y_2, z_2) S_{w_t w_t}(y_1, z_1, y_2, z_2, \omega) dz_1 dz_2 dy_1 dy_2 \tag{3.41}$$

$S_{w_t w_t}(y_1, z_1, y_2, z_2, \omega)$ is the cross-spectral density function for the wind load.

The variances of the response $X(t)$ and of the derivative of the response $\dot{X}(t)$ can then be calculated from

$$\sigma_X^2(y, z) = \frac{1}{2\pi} \sum_{m=1}^{\infty} \sum_{n=1}^{\infty} \Phi_m(y, z) \Phi_n(y, z) \int_0^{\infty} H_m^*(\omega) H_n(\omega) S_{P_m P_n}(\omega) d\omega \qquad (3.42)$$

$$\sigma_{\dot{X}}^2(y, z) = \frac{1}{2\pi} \sum_{m=1}^{\infty} \sum_{n=1}^{\infty} \Phi_m(y, z) \Phi_n(y, z) \int_0^{\infty} \omega^2 H_m^*(\omega) H_n(\omega) S_{P_m P_n}(\omega) d\omega \qquad (3.43)$$

If it can be assumed that only the N lowest modes contribute significantly to the response the double summations in (3.42) and (3.43) can be simplified

$$\sum_{m=1}^{\infty} \sum_{n=1}^{\infty} \rightsquigarrow \sum_{m=1}^{N} \sum_{n=1}^{N} \qquad (3.44)$$

Further, if it can be assumed that the eigen-frequencies are well separated then the cross-terms in in (3.42) and (3.43) can be neglected and the variances determined from

$$\sigma_X^2(y, z) \approx \frac{1}{2\pi} \sum_{m=1}^{\infty} \Phi_m^2(y, z) \int_0^{\infty} |H_m(\omega)|^2 S_{P_m P_m}(\omega) d\omega \qquad (3.45)$$

$$\sigma_{\dot{X}}^2(y, z) \approx \frac{1}{2\pi} \sum_{m=1}^{\infty} \Phi_m^2(y, z) \int_0^{\infty} \omega^2 |H_m(\omega)|^2 S_{P_m P_m}(\omega) d\omega \qquad (3.46)$$

If it also can be assumed that the structure is lightly damped and that the load is broadbanded then (3.45) and (3.46) can be simplified to

$$\sigma_X^2(y, z) \approx \frac{1}{8} \sum_{m=1}^{N} \Phi_m^2(y, z) \frac{S_{P_m P_m}(\omega_m)}{\zeta_m \omega_m^3 M_m^2} \qquad (3.47)$$

$$\sigma_{\dot{X}}^2(y, z) \approx \frac{1}{8} \sum_{m=1}^{N} \Phi_m^2(y, z) \frac{S_{P_m P_m}(\omega_m)}{\zeta_m \omega_m M_m^2} \qquad (3.48)$$

By the white-noise approximation (3.47) and (3.48) the back-ground turbulence contribution to the response is neglected, but a significant computational simplification is obtained.

3.2.2 Expected value function μ_X for response

The expected value of the response process $X(t)$ can be determined as the statically response of the structure with the statically wind load as load

$$\mu_X(y, z) \approx \sum_{m=1}^{N} \mu_{q_m}(y, z)\Phi_m(y, z) \tag{3.49}$$

Since the load is statically ($\dot{q}_m \approx \ddot{q}_m \approx 0$) it is seen that

$$\omega_m^2 \mu_{q_m} = \frac{1}{M_m} \int_0^h \int_0^d \Phi_m(y, z)w_s(y, z)dzdy \tag{3.50}$$

where $w_s(y, z)$ is the static wind load determined by

$$w_s(y, z) = q_m(z)C(y, z) \tag{3.51}$$

where $q_m(z)$:   10 min. mean wind velocity pressure at the height z.
        $C(y, z)$:   shape factor at the point (y, z).

$q_m(z)$ is determined from (3.67). Thus

$$\mu_X(y, z) \approx \sum_{m=1}^{N} \Phi_m(y, z)\frac{1}{\omega_m^2 M_m} \int_0^h \int_0^d \Phi_m(y, z)w_s(y, z)dzdy \tag{3.52}$$

Alternatively, $\mu_X(y, z)$ can be obtained from

$$\mu_X(y, z) = \int_0^h \int_0^d w_s(s, t)X_I(y, z, s, t)dsdt \tag{3.53}$$

where X_I is the influence function for the response given an unit load.

3.2.3 Approximations for $N = 1$ mode shape

If the response can be estimated with sufficient accuracy using only one mode shape, i.e. $N=1$ then the variance σ_X^2 can be determined from

$$
\begin{aligned}
\sigma_X^2(y, z) &= \frac{1}{2\pi} \Phi_1^2(y, z) \int_0^\infty |H_1(\omega)|^2 S_{P_1 P_1}(\omega) d\omega \\
&= \frac{1}{2\pi} \Phi_1^2(y, z) \int_0^\infty |H_1(\omega)|^2 \int_0^h \int_0^h \int_0^d \int_0^d \Phi_1(y_1, z_1) \Phi_1(y_2, z_2) \cdot \\
& \quad g(y_1, z_1) g(y_2, z_2) S_{u_x u_x}(y_1, z_1, y_2, z_2, \omega) dz_1 dz_2 dy_1 dy_2 d\omega \\
&\approx \frac{1}{2\pi} \Phi_1^2(y, z) |H_1(0)|^2 \int_0^\infty \int_0^h \int_0^h \int_0^d \int_0^d \Phi_1(y_1, z_1) \Phi_1(y_2, z_2) \cdot \\
& \quad g(y_1, z_1) g(y_2, z_2) S_{u_x u_x}(y_1, z_1, y_2, z_2, \omega) dz_1 dz_2 dy_1 dy_2 d\omega + \\
& \quad \frac{1}{2\pi} \Phi_1^2(y, z) \int_0^\infty |H_1(\omega)|^2 d\omega \int_0^h \int_0^h \int_0^d \int_0^d \Phi_1(y_1, z_1) \Phi_1(y_2, z_2) \cdot \\
& \quad g(y_1, z_1) g(y_2, z_2) S_{u_x u_x}(y_1, z_1, y_2, z_2, \omega_1) dz_1 dz_2 dy_1 dy_2 \\
&\approx (\mu_X(y, z) 2 I_u(z_{ref}))^2 (k_b + k_r)
\end{aligned} \tag{3.54}
$$

It should be noticed that the function $g(y, z) = \rho C(y, z) v_m(z)$. The background factor k_b and the resonance factor k_r are given by

$$
\begin{aligned}
k_b &= \frac{1}{2\pi} \frac{1}{\left(\int_0^h \int_0^d \Phi_1(y, z) g(y, z) dz dy\right)^2} \int_0^\infty \int_0^h \int_0^h \int_0^d \int_0^d \Phi_1(y_1, z_1) \Phi_1(y_2, z_2) \cdot \\
& \quad g(y_1, z_1) g(y_2, z_2) \frac{S_{u_x u_x}(y_1, z_1, y_2, z_2, \omega)}{\sigma_u^2} dz_1 dy_1 dz_2 dy_2 d\omega \\
&\approx \frac{1}{1 + 1.5 \sqrt{(\frac{d}{L(z_{ref})})^2 + (\frac{h}{L(z_{ref})})^2 + (\frac{d}{L(z_{ref})} \frac{h}{L(z_{ref})})^2}}
\end{aligned} \tag{3.55}
$$

$$
\begin{aligned}
k_r &= \frac{1}{8} \frac{\omega_1}{\zeta_1} \frac{1}{\left(\int_0^h \int_0^d \Phi_1(y, z) g(y, z) dz dy\right)^2} \int_0^h \int_0^h \int_0^d \int_0^d \Phi_1(y_1, z_1) \Phi_1(y_2, z_2) \cdot \\
& \quad g(y_1, z_1) g(y_2, z_2) \frac{S_{u_x u_x}(y_1, z_1, y_2, z_2, \omega_1)}{\sigma_u^2} dz_1 dz_2 dy_1 dy_2 \\
&\approx \frac{1}{2} \frac{\pi^2}{\delta_s + \delta_a} \frac{n_1 S_{u_x}(z_{ref}, n_1)}{\sigma_u^2} K_s(n_1)
\end{aligned} \tag{3.56}
$$

where

$$K_s(n_1) = \frac{\int_0^h \int_0^h \int_0^d \int_0^d \Phi_1(y_1, z_1)\Phi_1(y_2, z_2)g(y_1, z_1)g(y_2, z_2)\sqrt{Coh_{u_x u_x}(y_1, z_1, y_2, z_2, \omega_1)}dz_1 dz_2 dy_1}{\left(\int_0^h \int_0^d \Phi_1(y, z)g(y, z)dzdy\right)^2}$$

(3.57)

The variance $\sigma_{\dot{X}}^2$ can similarly be determined by from

$$
\begin{aligned}
\sigma_{\dot{X}}^2(z) &= \frac{1}{2\pi}\Phi_1^2(y, z)\int_0^\infty \omega^2|H_1(\omega)|^2 S_{P_1 P_1}(\omega)d\omega \\
&= \frac{1}{2\pi}\Phi_1^2(y, z)\int_0^\infty \omega^2|H_1(\omega)|^2 \int_0^h \int_0^h \int_0^d \int_0^d \omega^2\Phi_1(y_1, z_1)\Phi_1(y_2, z_2) \cdot \\
&\quad g(y_1, z_1)g(y_2, z_2)S_{u_x u_x}(y_1, z_1, y_2, z_2, \omega)dz_1 dz_2 dy_1 dy_2 d\omega \\
&\approx \frac{1}{2\pi}\Phi_1^2(y, z)|H_1(0)|^2 \int_0^\infty \int_0^h \int_0^h \int_0^d \int_0^d \Phi_1(y_1, z_1)\Phi_1(y_2, z_2) \cdot \\
&\quad g(y_1, z_1)g(y_2, z_2)S_{u_x u_x}(y_1, z_1, y_2, z_2, \omega)dz_1 dz_2 dy_1 dy_2 d\omega + \\
&\quad \frac{1}{2\pi}\Phi_1^2(y, z)\int_0^\infty \omega^2|H_1(\omega)|^2 d\omega \int_0^h \int_0^h \int_0^d \int_0^d \Phi_1(y_1, z_1)\Phi_1(y_2, z_2) \cdot \\
&\quad g(y_1, z_1)g(y_2, z_2)S_{u_x u_x}(y_1, z_1, y_2, z_2, \omega_1)dz_1 dz_2 dy_1 dy_2 \\
&\approx (\mu_X(y, z)2I_u(z_{ref}))^2(k_{\dot{b}} + k_{\dot{r}})
\end{aligned}
$$

(3.58)

where the factors $k_{\dot{b}}$ and $k_{\dot{r}}$ are given by

$$
\begin{aligned}
k_{\dot{b}} &= \frac{1}{2\pi}\frac{1}{\left(\int_0^h \int_0^d \Phi_1(y, z)g(y, z)dzdy\right)^2}\int_0^\infty \int_0^h \int_0^h \int_0^d \int_0^d \omega^2\Phi_1(y_1, z_1)\Phi_1(y_2, z_2) \cdot \\
&\quad g(y_1, z_1)g(y_2, z_2)\frac{S_{u_x u_x}(y_1, z_1, y_2, z_2, \omega)}{\sigma_u^2}dz_1 dz_2 dy_1 dy_2 d\omega
\end{aligned}
$$

(3.59)

$$
\begin{aligned}
k_{\dot{r}} &= \frac{1}{8}\frac{\omega_1^3}{\zeta_1}\frac{1}{\left(\int_0^h \Phi_1(y, z)g(y, z)dydz\right)^2}\int_0^h \int_0^h \int_0^d \int_0^d \Phi_1(y_1, z_1)\Phi_1(y_2, z_2) \cdot \\
&\quad g(y_1, z_1)g(y_2, z_2)\frac{S_{u_x u_x}(y_1, z_1, y_2, z_2, \omega_1)}{\sigma_u^2}dz_1 dz_2 dy_1 dy_2
\end{aligned}
$$

(3.60)

3.2.4 General approximations for N mode shapes

If the response is estimated using N mode shapes σ_X^2 can be determined by

$$
\begin{aligned}
\sigma_X^2(y,z) &= \frac{1}{2\pi} \sum_{m=1}^{N} \sum_{n=1}^{N} \Phi_m(y,z)\Phi_n(y,z) \int_0^\infty H_m^*(\omega)H_n(\omega) \int_0^h \int_0^h \int_0^d \int_0^d \Phi_m(y_1,z_1)\Phi_m(y_2,z_2 \\
&\quad g(y_1,z_1)g(y_2,z_2)S_{u_x u_x}(y_1,z_1,y_2,z_2,\omega)dz_1 dz_2 dy_1 dy_2 d\omega \\
&\approx \frac{1}{2\pi} \sum_{m=1}^{N} \Phi_m^2(y,z)|H_m(0)|^2 \int_0^\infty \int_0^h \int_0^h \int_0^d \int_0^d \Phi_1(y_1,z_1)\Phi_1(y_2,z_2) \cdot \\
&\quad g(y_1,z_1)g(y_2,z_2)S_{u_x u_x}(y_1,z_1,y_2,z_2,\omega)dz_1 dz_2 dy_1 dy_2 d\omega + \\
&\quad \frac{1}{2\pi} \sum_{m=1}^{N} \Phi_m^2(y,z) \int_0^\infty |H_m(\omega)|^2 d\omega \int_0^h \int_0^h \int_0^d \int_0^d \Phi_1(y_1,z_1)\Phi_1(y_2,z_2) \cdot \\
&\quad g(y_1,z_1)g(y_2,z_2)S_{u_x u_x}(y_1,z_1,y_2,z_2,\omega_m)dz_1 dz_2 dy_1 dy_2 \\
&\approx (\mu_X(y,z)2I_u(z_{ref}))^2(k_b + k_{r_1} + \ldots + k_{r_N})
\end{aligned}
\tag{3.61}
$$

where the background factor k_b and the resonance factor k_{r_m} are given by

$$
\begin{aligned}
k_b &= \frac{1}{2\pi} \frac{1}{\left(\sum_{m=1}^{N} \int_0^h \int_0^d \Phi_m(y,z)g(y,z)dzdy\right)^2} \sum_{m=1}^{N} \int_0^\infty \int_0^h \int_0^h \int_0^d \int_0^d \Phi_m(y_1,z_1)\Phi_m(y_2,z_2 \\
&\quad g(y_1,z_1)g(y_2,z_2)\frac{S_{u_x u_x}(y_1,z_1,y_2,z_2,\omega)}{\sigma_u^2}dz_1 dz_2 dy_1 dy_2 d\omega
\end{aligned}
\tag{3.62}
$$

$$
\begin{aligned}
k_{r_m} &= \frac{1}{8} \frac{\omega_m}{\zeta_m} \frac{1}{\left(\sum_{m=1}^{N} \int_0^h \int_0^d \Phi_m(y,z)g(y,z)dzdy\right)^2} \int_0^h \int_0^h \int_0^d \int_0^d \Phi_m(y_1,z_1)\Phi_m(y_2,z_2) \cdot \\
&\quad g(y_1,z_1)g(y_2,z_2)\frac{S_{u_x u_x}(y_1,z_1,y_2,z_2,\omega_m)}{\sigma_u^2}dz_1 dz_2 dy_1 dy_2
\end{aligned}
\tag{3.63}
$$

The variance $\sigma_{\dot{X}}^2$ can be determined similarly.

3.2.5 Equivalent quasi-static wind load

Equivalent quasi-static wind load can be defined by

$$
w_e(y,z) = (1 + 2k_p I_u(z))\sqrt{k_b + k_{r_1} + \ldots + k_{r_N}}\, w_s(y,z)
\tag{3.64}
$$

3.3 DS410, Along-wind load

The following section outlines the rules for calculation of the dynamic along-wind load in the Danish code for loads on structures (DS410), [1].

The characteristic along-wind load F_w on a structure with a given reference area A_{ref}, see section 6.2 in [1], can be estimated according to DS410 if the following assumptions are fulfilled:

- The structure should correspond to the one of the standardized cases shown in figure 3.1.

- The along-wind load is determined from the undisturbed wind field.

- Only one eigen-mode is important, namely the one with the lowest eigen-frequency.

- The along-wind eigen-mode is decoupled from the other eigen-modes.

- The structure behaves in a linear-elastic manner with viscous damping.
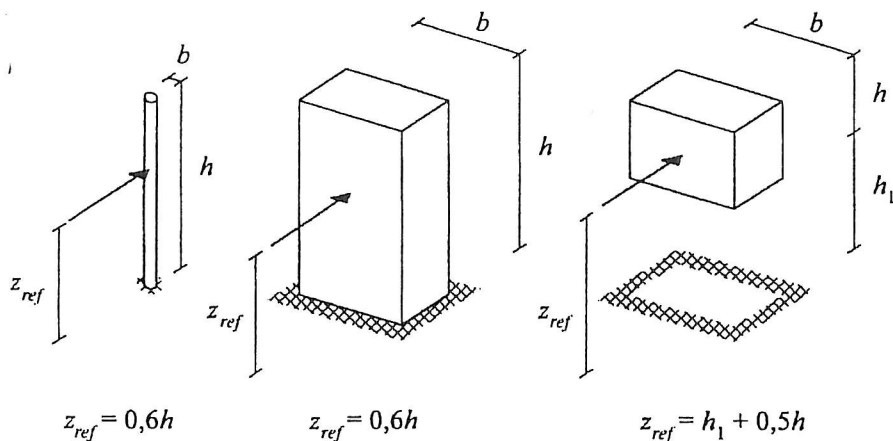
Figure 3.1: *The reference height z_{ref} for structures considered in* [1].

The characteristic along-wind load F_w is given as for a structure with the reference area A_{ref}

$$F_w(z) = q_{max}(z)c_d c_f A_{ref} \tag{3.65}$$

where c_f is the shape factor. The maximal characteristic wind pressure is

$$q_{max}(z) = (1 + 7I_v(z))q_m(z) \tag{3.66}$$

The mean wind pressure is given by

$$q_m(z) = \frac{1}{2}\rho v_m^2(z) \tag{3.67}$$

where the mean wind velocity follows from

$$v_m(z) = v_b k_t \ln\left(\frac{z}{z_0}\right) \tag{3.68}$$

The turbulence intensity $I_v(z)$ is given by

$$I_v(z) = \frac{1}{\ln\left(\dfrac{z}{z_0}\right)} \tag{3.69}$$

c_d is the dynamic coefficient

$$c_d = \frac{1 + 2k_p I_v(z_{ref})\sqrt{k_b + k_r}}{1 + 7I_v(z_{ref})} \tag{3.70}$$

which is defined as the ratio between the dynamic value of the response due the turbulence load and the quasi-static load, respectively. Therefore c_d is proportional to the gust factor ϕ_X defined in (2.2). In DS410 the peak factor k_p is given by

$$k_p = \sqrt{2\ln(\nu T)} + \frac{0.577}{\sqrt{2\ln(\nu T)}} \quad , T = 600 \text{ s} \tag{3.71}$$

The mean up-crossing rate ν used in (3.71) is estimated by

$$\nu = \frac{1}{2\pi}\frac{\sigma_{\dot{X}}}{\sigma_X} \approx \sqrt{\frac{n_0^2 k_b + n_1^2 k_r}{k_b + k_r}} \tag{3.72}$$

where n_0 is an estimate of the mean up-crossing rate for a structure where dynamic effects are negligible, i.e. outcrossing due to quasi-static wind induced response. n_1 is the first natural frequency. n_0 is estimated by

$$n_0 = 0.3\frac{v_m(z_{ref})}{\sqrt{hd}}\sqrt{\frac{\sqrt{hd}}{L(z_{ref})}} \quad \text{for } n_0 \leq 0.42\text{Hz and} \quad n_0 \leq n_1 \tag{3.73}$$

The length scale L is given by

$$
\begin{aligned}
L(z) &= 100\left(\frac{z}{10}\right)^{0.3} \quad \text{for } z \geq z_{min} \\
L(z) &= L(z_{min}) \quad \text{for } z < z_{min}
\end{aligned} \tag{3.74}
$$

The background response factor k_b and the resonance response factor k_r used in DS410 follows from (3.55) and (3.56), i.e

$$k_b = \frac{1}{1 + \dfrac{3}{2}\sqrt{\left(\dfrac{d}{L(z_{ref})}\right)^2 + \left(\dfrac{h}{L(z_{ref})}\right)^2 + \left(\dfrac{d}{L(z_{ref})}\dfrac{h}{L(z_{ref})}\right)^2}} \tag{3.75}$$

and

$$k_r = \frac{1}{2} \frac{\pi^2}{\delta_s + \delta_a} \frac{n_1 S_{u_x}(z_{ref}, n_1)}{\sigma_u^2} K_s(n_1) \qquad (3.76)$$

where $n_1 = \dfrac{\omega_1}{2\pi}$:   is the eigen-frequency.

       $\delta_s = 2\pi\zeta_{1s}$:   is the structural damping coefficient for lowest eigen-frequency.

       $\delta_a = 2\pi\zeta_{1a}$:   is the aerodynamic damping coefficient for lowest eigen-frequency.

       $K_s(n_1)$:   is the size reduction factor given by.

The size reduction factor follows from (3.57)

$$K_s(n) = \frac{\displaystyle\int_0^h \int_0^h \int_0^d \int_0^d \Phi_1(y_1, z_1)\Phi_1(y_2, z_2)g(y_1, z_1)g(y_2, z_2)K(y_1, z_1, y_2, z_2, n)dz_1 dz_2 dy_1 dy_2}{\displaystyle\int_0^h \int_0^d \int_0^h \int_0^d \Phi_1(y_1, z_1)g(y_2, z_2)\Phi_1(y_1, z_1)g(y_2, z_2)dz_1 dy_1 dz_2 dy_2}$$

$$(3.77)$$

Assuming $g(y, z) = g_y(y)g_z(z)$ implies that $K_s(n)$ can be approximately estimated by

$$K_s(n) = \frac{1}{1 + \sqrt{(G_y\phi_y)^2 + (G_z\phi_z)^2 + \left(\dfrac{2}{\pi}G_y\phi_y G_z\phi_z\right)^2}} \qquad (3.78)$$

where $G_y = G$ in table 3.1 with $g_y(y) \propto g_\alpha(\alpha)$ and $\alpha = y/h$

       $G_z = G$ in table 3.1 with $g_z(z) \propto g_\alpha(\alpha)$ and $\alpha = z/d$

       $\phi_y = c_y bn/v_m(z_{ref})$, $c_y = 10$

       $\phi_z = c_z dn/v_m(z_{ref})$, $c_z = 10$

$g_\alpha(\alpha)$:	1	α	α^2	$\sin(\pi\alpha)$
G :	$1/2$	$3/18$	$5/18$	$4/\pi^2$

Table 3.1: G_y and G_z.

DS410 [1] specifies for two points (z_1, y_1) and (z_2, y_2) on a surface the following normalized co-spectrum

$$K(z_1, z_2, y_1, y_2, \omega) = \sqrt{Coh_{u_x u_x}(y_1, z_1, y_2, z_2, \omega_1)} = \exp\left(-\frac{\omega}{2\pi} \frac{\sqrt{c_y^2(y_1 - y_2)^2 + c_z^2(z_1 - z_2)^2}}{1/2(v(z_1) + v(z_2))}\right)$$

$$(3.79)$$

where $c_z = c_y = 10$. In accordance with [1], the phase-spectrum is on the safe side neglected in estimation of the dynamic response due to wind turbulence.

The aerodynamic damping is given by the logarithmic decrement

$$\delta_a = \frac{c_f \rho v_m(z_{ref})}{2n_1 \mu_{ref}} \tag{3.80}$$

where the reference mass μ_{ref} for the structure is

$$\mu_{ref} = \frac{\int_0^h \int_0^b \mu(y,z)\Phi_1^2(y,z)dydz}{\int_0^h \int_0^b \Phi_1^2(y,z)dydz} \tag{3.81}$$

The structural damping given as a logarithmic decrement is obtained from

$$\delta_s = a_1 n_1 + b_1 \geq \delta_{min} \quad n_1 \leq 3\text{Hz} \tag{3.82}$$

where a_1, b_1 and δ_{min} is given in table 3.2

Type of Structure	$a_1[\text{s}]$	b_1	δ_{min}
concrete structure	0.045	0.05	0.10
steel structure	0.045	0	0.05
concrete chimney	0.075	0	0.03
steel chimney	0	0.015	0

Table 3.2: *Structural damping coefficients.*

3.4 Example 1: Along-wind load on chimney

The following example demonstrates the application of the rules in DS410 [1] for calculation of the dynamic along-wind load on a steel chimney. The maximal displacement $x_{max}(z = h)$ and the maximal moment $M_{max}(z = 0)$ will be compared with results obtained from the stochastic response analysis equations in section 3.1.

The structural data [2] for the steel chimney are as follows

height :	$h = 50$ m
external diameter :	$b = 1$ m
total mass per unit height :	$\mu = 3498$ kg/m
1st natural frequency :	$n_1 = 0.34$ Hz.
2nd natural frequency :	$n_2 = 1.91$ Hz.
structural damping :	$\delta_s = 0.015$.
shape factor :	$c_f = 0.733$ (DS410)

The chimney is assumed to be located in an area with a roughness length $z_0 = 0.05$ m and a terrain factor $k_t = 0.19$. Further, the basic wind velocity for this area is chosen as $v_b = 27$

m/s and the air density is ρ=1.25 kg/m^3. Tables 3.3 and 3.4 show the results based on the rules in DS410 and from a stochastic response analysis where $N = 1$ and $N = 2$ have been considered. It is seen that the estimated values based on DS410 correspond very well to the results from the stochastic response analysis. DS410 gives conservative results. Further, it is seen from table 3.4 that the main part of the response is due to the first mode. This is also seen from figure 3.2 where the auto-spectral density function $S_{XX}(w)$ for displacement response at $z = 50$ m is shown as a function of cyclic frequency ω.

Variable	$N = 1$
A_{ref}	$50\ m^2$
$L(z_{ref})$	$139\ m$
$R(z_{ref}, n_s)$	0.099
k_b	0.649
$K_s(n_1)$	0.409
δ_s	0.015
δ_a	0.012
k_r	7.508
n_0	$0.314\ Hz.$
ν	$0.338\ Hz.$
k_p	3.437
I_v	0.156
c_d	1.943
φ_X	4.061
F_w	$1.051 \cdot 10^5 N/m^2$
x_{max}	$0.211\ m$
M_{max}	$2.642 \cdot 10^6 Nm$

Table 3.3: *Along-wind response obtained using rules in DS410* [1].

Variable	N = 1	N = 2
μ_x	$0.047\ m$	$0.047\ m$
k_b	0.591	—
k_r	7.503	—
σ_x	$0.041\ m$	$0.041\ m$
k_p	3.431	—
x_{max}	$0.186\ m$	$0.188\ m$
μ_M	$6.051 \cdot 10^5\ Nm$	$6.441 \cdot 10^5\ Nm$
σ_M	$5.193 \cdot 10^5\ Nm$	$5.495 \cdot 10^5\ Nm$
k_p	3.431	—
M_{max}	$2.389 \cdot 10^6\ Nm$	$2.546 \cdot 10^6\ Nm$

Table 3.4: *Along-wind response obtained using stochastic response analysis.*
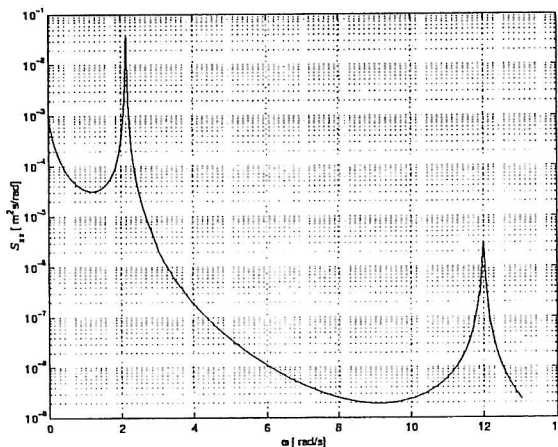

Figure 3.2: *Auto-spectral density function $S_X X(w)$ for displacement response at $z = 50$ m.*

Chapter 4

Across-wind load

The preceding chapters described the models for along-wind load and response caused by the natural turbulence in the wind flow. However, the structure itself may change the wind flow pattern and thereby response due to the changed wind flow can be obtained. Of these, the most important phenomenon is vibrations generated by the vortex shedding. Slender structures such as chimneys, towers, electrical transmission lines or bridge-decks can have a formation of vortices in the wake flow which in rare cases causes significant vibrations of the structure.

In this chapter vortex induced vibrations of one-dimensional slender structures will be considered with a coordinate system with the x-axis in the along-wind direction, the y-axis perpendicular to the wind direction, designated the across-wind direction, and the z-axis in the longitudinal direction of the structure. The structure will vibrate due to the turbulence components $u_x(z, t)$ and $u_y(z, t)$. In the across-wind direction the structure will be excitated by a force caused of the $u_y(z, t)$ and a force due to vortex shedding which generates a across-wind force [14]. When the dominant frequency of the vortex shedding is equal to the lowest natural frequency of the structure significant across-wind vibrations can be produced. Normally the vibrations due to vortex shedding occur for a mean wind velocity lower than the mean wind velocity which is significant for the quasi-static design wind load. The vortex induced vibrations can cause fatigue failure of e.g. a steel chimney.

Generally, the across-wind loading can be divided into the following three groups:

- Wind load due to the turbulence component $u_y(z, t)$.

- Wind load due to vortex shedding.

- Wind induced vibration load.

In the following sections the physical reasons for these different type of across-wind load will be described and calculation models for the load and related response will be presented.

40

4.1 Across-wind response

When a slender structure vibrates with the velocities $\dot{x}(z,t)$ and $\dot{y}(z,t)$, the following relative velocity is obtained, see figure 4.1,

$$v_{rel}^2(z,t) = \big(v(z) + u_x(z,t) - \dot{x}(z,t)\big)^2 + \big(u_y(z,t) - \dot{y}(z,t)\big)^2 \tag{4.1}$$

where
$v(z)$	:	the mean wind velocity in the along-wind direction.
$u_x(z,t)$	:	the turbulence component in the along-wind direction.
$\dot{x}(z,t)$	:	the velocity of the structure in the along-wind direction.
$u_y(z,t)$	:	the turbulence component in the across-wind direction.
$\dot{y}(z,t)$	:	the velocity of the structure in the along-wind direction.

By using the same assumption as in the Davenport wind load model for quasi-static aerodynamic, the wind load per unit length $p_x(z,t)$ can is given by, [8]

$$
\begin{aligned}
p_x(z,t) &= \frac{1}{2}\rho C_D(z)d(z)v_{rel}^2(z,t)\cos\theta \\
&= \frac{1}{2}\rho C_D(z)d(z)v_{rel}(z,t)(v(z) + u_x(z,t) - \dot{x}(z,t))
\end{aligned}
\tag{4.2}
$$

$$
\begin{aligned}
p_y(z,t) &= \frac{1}{2}\rho C_D(z)d(z)v_{rel}^2(z,t)\sin\theta \\
&= \frac{1}{2}\rho C_D(z)d(z)v_{rel}(z,t)(u_y(z,t) - \dot{y}(z,t))
\end{aligned}
\tag{4.3}
$$

where $\sin\theta$ and $\cos\theta$ is given in figure 4.1

$$
\begin{aligned}
\sin\theta &= \frac{u_y(z,t) - \dot{y}(z,t)}{v_{rel}(z,t)} \\
\cos\theta &= \frac{v(z) + u_x(z,t) - \dot{x}(z,t)}{v_{rel}(z,t)}
\end{aligned}
\tag{4.4}
$$

Assuming that the mean wind velocity $v(z)$ is the most significant component the wind load in the x-direction can be written following (1.10)

$$p_x(z,t) = p_x^s(z) + p_x^v(z,t) - p_x^a(z,t) \tag{4.5}$$
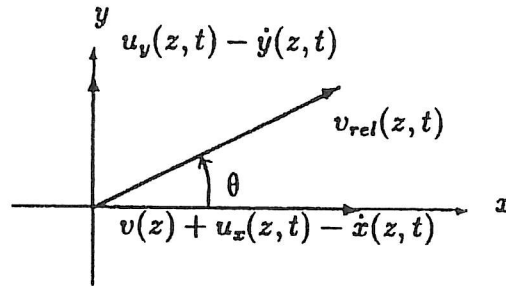
Figure 4.1: *Definition of θ.*

where $\quad p_x^s(z) \quad = \quad \frac{1}{2}g(z)v(z) \quad$: quasi-static load from $v(z)$.

$\qquad\quad p_x^v(z,t) \quad = \quad g(z)u_x(z,t) \quad$: wind load in the along-wind direction.

$\qquad\quad p_x^a(z,t) \quad = \quad g(z)\dot{x}(z,t) \quad$: aerodynamic wind load in the along-wind direction.

$\qquad\quad g(z) \qquad\quad = \quad \rho v(z)d(z)C_D(z) \quad$: transfer function.

and in the y-direction

$$p_y(z,t) = p_y^v(z,t) - p_y^a(z,t) \tag{4.6}$$

where $\quad p_y^v(z,t) \quad = \quad \frac{1}{2}g(z)u_y(z,t) \quad$: turbulence wind load in the across-wind direction.

$\qquad\quad p_y^a(z,t) \quad = \quad \frac{1}{2}g(z)\dot{y}(z,t) \quad$: aerodynamic wind load in the across-wind direction.

From (4.6) it is seen that the aerodynamic component in the y-direction has half the intensity as the corresponding component in the x-direction. The aerodynamic damping ratio in the across-wind direction for the m'th eigen mode is then given as (cf. (1.30))

$$\zeta_m^a = \frac{1}{4M_m\omega_m}\int_0^h \rho v(z)d(z)C_D(z)\Phi_m^2(z)dz \tag{4.7}$$

Φ_m is the m'th mode shape belonging to bending vibrations in the across-wind direction. The aerodynamic loading per unit length is taking into account as a part of the total damping.

The total wind loading per unit length in the y-direction is

$$p_y(z,t) = p_y^v(z,t) + p_y^h(z,t) \tag{4.8}$$

where the vortex induced wind load per unit length is given as $p_y^h(z,t)$. The component $p_y^v(z,t)$ is broad-banded while the component $p_y^h(z,t)$ is narrow-banded. The two components can normally be modelled as independent Gaussian processes implying that the cross-spectral density is obtained as

$$S_{p_yp_y}(z_1,z_2,\omega) = S_{p_y^vp_y^v}(z_1,z_2,\omega) + S_{p_y^hp_y^h}(z_1,z_2,\omega) \tag{4.9}$$

For a height 100-200 m over a homogeneous terrain the standard deviations of the turbulence components are estimated as [2]

$$\sigma_{u_x} = Av_*, \qquad \sigma_{u_y} = \frac{3}{4}Av_*, \qquad \sigma_{u_z} = \frac{1}{2}Av_*, \qquad A \approx 2.5 \tag{4.10}$$

which means that the auto-spectral densities of the components u_y and u_z are given by

$$S_{u_y}(z,\omega) \approx (0.75)^2 S_{u_x}(z,\omega) \tag{4.11}$$
$$S_{u_z}(z,\omega) \approx (0.50)^2 S_{u_x}(z,\omega) \tag{4.12}$$

The estimation of the structural response due to u_y and u_z can be done similar to the response estimation due to the mean along-wind load if the cross-spectral density $S_{w_t w_t}(z_1, z_2, \omega)$ is changed to the cross-spectral density $S_{p_y^v p_y^v}(z_1, z_2, \omega)$, given by

$$S_{p_y^v p_y^v}(z_1, z_2, \omega) \approx (0.375)^2 S_{w_t w_t}(z_1, z_2, \omega) \tag{4.13}$$

It should be noticed that [8] points out that the structural response due to u_y and u_z normally will be smaller than the the structural response due to vortex shedding. In chapter 5 $S_{p_y^h p_y^h}(z_1, z_2, \omega)$ will be considered.

4.2   Vortex shedding at stationary cylinder

The across-wind load introduced for flow past a cylinder can be divided into whether the cylinder is stationary or moving. In this section flow around a stationary cylinder is considered while flow around a moving cylinder is considered in the following section.

Flow around a cylinder generates a boundary layer due to the viscosity of the air. For increasing values of the Reynolds number Re, given by (4.14) the boundary layer changes characteristics and break away at the separation points at the surface of the cylinder.

$$Re = \frac{v \cdot d}{\nu} \tag{4.14}$$

where ν is the kinematic viscosity. Figure 4.2 shows the flow around a stationary cylinder for increasing values of the Reynolds number.

$\underline{0 \leq Re < 5}$: Flow like a potential flow since no boundary layer will be developed at such a low flow velocity.

$\underline{5 \leq Re < 50}$: A laminar boundary layer is developed. The gradient of the pressure along the flow direction has a magnitude corresponding to a shed of symmetrical vortices.
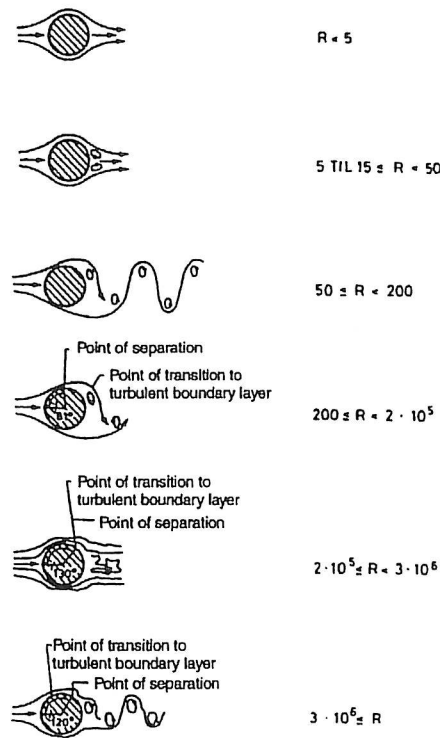
Figure 4.2: *Vortex shedding for flow past a stationary cylinder*, [14].

$\underline{50 \leq Re < 200}$: Separation points are located at the front of the cylinder. Vortices are shed alternately from one side then the other. The dominant frequency of the vortex shedding is given by

$$n_s = \frac{S_t \cdot v}{d} \tag{4.15}$$

where S_t is the non-dimensional *Strouhal number*, $(S_t \approx 0.2)$. The vortices create a pattern in their wake often referred to as the *von Karman trail*. The vortices are laminar and harmonically varying.

$\underline{200 \leq Re < 2 \cdot 10^5}$: A subcritical region where the wake and each vortex now are turbulent while the boundary layer is laminar and the vortex shedding is still harmonically varying.

$\underline{2 \cdot 10^5 \leq Re < 3 \cdot 10^6}$: A supercritical region with a turbulent boundary layer and a non-harmonically varying vortex shedding.

$\underline{3 \cdot 10^6 \leq Re}$: A transcritical region with a turbulent boundary layer and now a nearly harmonically varying vortex shedding.

Vortex shedding will give rise to a lift or across-wind force with a shedding frequency n_s. Normally, high chimneys with a circular cross section are in the supercritical or transcritical regions, see figure 4.3.
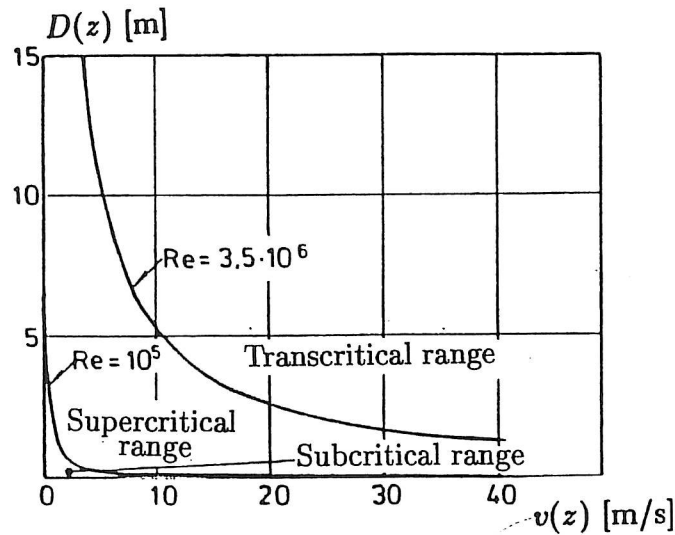
Figure 4.3: *Diagram for determining of the flow type around a structure with a circular cross section,* [8].

4.3 Vortex shedding at moving cylinder

For a cylinder with a smooth surface the vortex induced wind loading per unit length is approximately given by

$$p_y^h(z,t) = \frac{1}{2}\rho v^2(z)d(z)C_L(z,t) \tag{4.16}$$

where C_L is a so-called lift coefficient

$$C_L = C_L\big(M_r, S_c, V_r, Re, Y/D, \text{turbulensintensity}\big) \tag{4.17}$$

where M_r = $\frac{\mu_e}{\rho D^2}$:   the reduced mass ratio.
S_c = $4\pi M_r \zeta_k$:   the Scruton number.
V_r = $\frac{v}{D n_0}$:   the reduced velocity.

μ_e is a measure of the structural mass per unit height, n_0 is the natural frequency of the structural system , and D is a typical diameter. Y is the vibration amplitude and therefore is Y/D named the vibration level. M_r is a measure of the ratio between the structural mass and the mass of the displaced medium S_c is a non-dimensional measure of the structural internal damping.
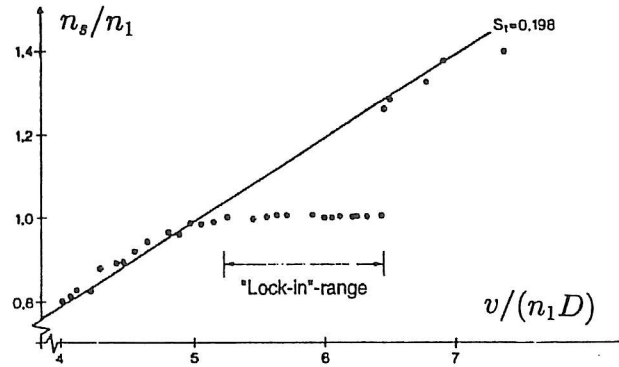
Figure 4.4: *Lock-in effect for moving cylinder,* [2].

Based on experiments the following can be stated [12,13,14,17,18]:

- For $V_r < 4.75$ the vibration level is small and vortex shedding occurs at the Strouhals frequency, (see figure 4.4).

- From $V_r \sim 4.75$ and up to $V_r \sim 8$ vortex shedding occurs at the natural frequency n_0. Resonance in this region generates vibration of the cylinder which influences on the wind field. For increasing amplitude a more pronounced effect will be seen and the natural frequency of the cylinder dictates the the frequency of vortex shedding. This phenomenon is referred to as a *lock-in* because the shedding frequency is locked into the natural frequency of the structure. The lock-in continues over a frequency band followed by frequency region where the Strouhal relation (4.15) again applies for V_r larger than ~ 8. (see figure 4.4).

- The lock-in interval depends on the structural damping.

- The motion of the cylinder causes a synchronizing of the vortex shedding along the length of the cylinder. The correlation length of the vortex induced loading is significantly increased with the vibration level. Therefore the lock-in phenomenon has a self induced effect and explains the increase in wind load magnitude at lock-in [18]. In figure 4.5 the correlation coefficient $\rho_{p_y^h p_y^h}$ between the lift force per unit length at two cross sections with the distance l defined by (4.18) shown as a function of the vibration level.

$$\rho_{p_y^h p_y^h} = \frac{E[p_y^h(z)\, p_y^h(z+l)]}{\sigma_{p_y^h}(z)\, \sigma_{p_y^h}(z+l)} \qquad (4.18)$$

- At a vibration level $Y/D \approx 0.5$ the wind loading may be fully correlated along the cylinder. For an increasing vibration level the lift coefficient starts to decrease and will be disappeared for $Y/D \sim 1.5 - 2$. This happens because the vortex shedding becomes irregular and more than two vortices are shed for each vibration period. Therefore the vortex induced vibrations are self-limited, [12].

- The vibration level decreases when the Scruton number increases. Scruton developed a simple method which can be used to evaluate the response for lock-in of structures with a cylindrical cross section, [2]

for $S_c > 20$: no risk for lock-in.

$S_c < 10$: risk for lock-in.

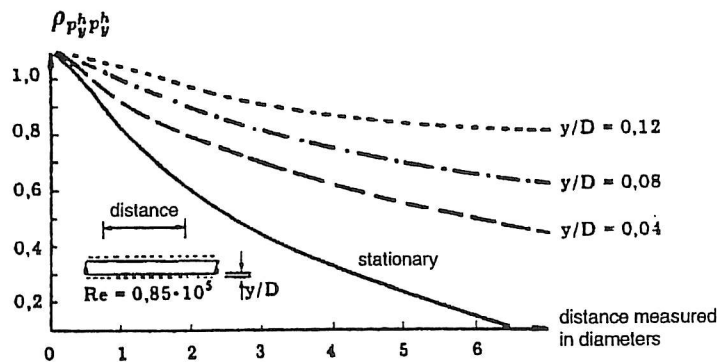$10 < S_c < 20$: transition region where lock-in can occur.

Figure 4.5: *Correlation as a function of the distance between two points for different vibration levels , [12].*

4.3.1   Vortex shedding in natural wind

Due to the turbulence in the natural wind the across-wind load has more than one frequency n_s. Turbulence with vortex extent larger than $10 \cdot D$ is defined as u' and can be considered as a slowly variation of the mean wind velocity. If this turbulence term is taken into account in the Strouhal relation (4.15) it is seen that vortex shedding at a stationary cylinder occurs in the frequency band $n_s + n'_s$

$$n_s + n'_s = \frac{S_t \cdot (v + u')}{d} \qquad (4.19)$$

The turbulence also has the effect that the auto-spectra of the across-wind force includes two peaks; one from the vortex shedding and one from the resonance with the structural frequency. For a vortex shedding frequency close to the structural frequency only one peak will be seen in the auto-spectrum due to the lock-in phenomenon (see figure 4.6).
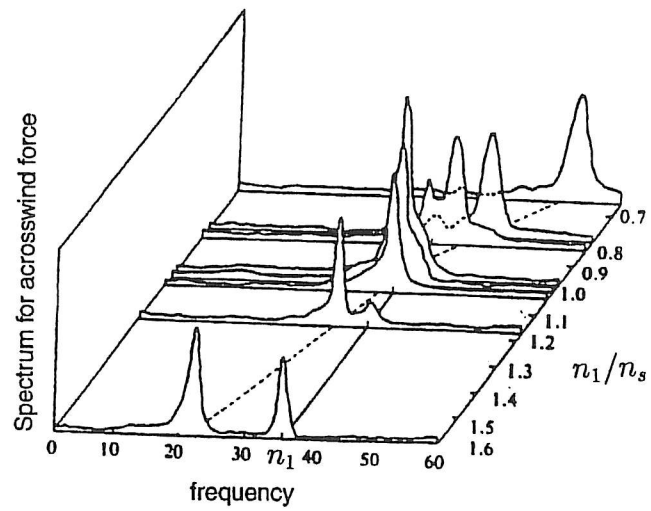
Figure 4.6: *Auto-spectrum for across-wind force as a function of the shedding frequency and the natural frequency,* [13].

Chapter 5

Dynamic response of structures due to across-wind load

The following section outlines a stochastic model for estimation of the vortex induced wind load.

5.1 Stochastic model for vortex induced wind load

The across-wind load due to vortex shedding can be written

$$p_y^h(z,t) = \frac{1}{2}\rho v^2(z)d(z)C_L(z,t) = h(z)C_L(z,t) \tag{5.1}$$

The lift coefficient C_L is a non-dimensional stochastic process with mean value 0. The cross-spectral density then becomes

$$S_{p_y^h p_y^h}(z_1, z_2, \omega) = h(z_1)h(z_2)S_{C_L C_L}(z_1, z_2, \omega) \tag{5.2}$$

where

$$S_{C_L C_L}(z_1, z_2, \omega) = \sqrt{S_{C_L}(z_1, \omega)}\sqrt{S_{C_L}(z_2, \omega)}\sqrt{Coh_{C_L}(z_1, z_2, \omega)}\cos(\Phi_{C_L}(z_1, z_2, \omega)) \tag{5.3}$$

From experiments made in the subcritical region of Re the following expression has been proposed for the auto-spectral density of the lift coefficient, [20].

$$S_{C_L}(z, \omega) = \frac{2\pi\sigma_{C_L}^2(z)}{\sqrt{\pi}B(z)\omega_s}\exp\left[-\left(\frac{\omega - \omega_s}{B(z)\omega_s}\right)^2\right] \tag{5.4}$$

49

where σ_{C_L} : standard deviation of the lift coefficient .

$B(z)$: spectral width.

ω_s : cyclic vortex shedding frequency.

It should be noticed that the auto-spectrum may be is approximated by a Gaussian spectrum since the wind velocity $v(z) + u_x(z,t)$ in the wind direction is approximately Gaussian with mean value $v(z)$.

The spectral width $B(z) = \sqrt{2}(\sigma_v(z)/v(z))$ is a measure of the relative width of the peak in the spectrum around ω_s and states the band of frequencies where vortex shedding occurs. $B(z)$ is proportional to the intensity of turbulence $\sigma_v(z)/v(z)$. Since the spectrum of the lift coefficient C_L in a laminar flow (i.e. $\sigma_v(z) \to 0$) has a final width the spectral width becomes, [19]

$$B^2(z) = B_0^2 + 2\left(\frac{\sigma_v(z)}{v(z)}\right)^2 \qquad \text{where} \quad B_0 = [0,05 - 0,1] \tag{5.5}$$

The standard deviation of the wind velocity σ_v is generally given by, see table 1.1

$$\sigma_v \approx \sqrt{6}v_* = \sqrt{6}v_b k_t \kappa \tag{5.6}$$

where κ : the von Karmann constant $= 0.408$.

v_b : the basic wind velocity

k_t : terrain parameter.

v_* : friction velocity.

The coherence Coh_{C_L} and the phase Φ_{C_L} spectra are only important around the spectral peak and can be estimated as, [20]

$$Coh_{C_L}(z_1, z_2, \omega) = \left[\exp\left(-ar^2\right)\right]^2 \tag{5.7}$$

$$\Phi_{C_L}(z_1, z_2, \omega) = br \tag{5.8}$$

where

$$r = \frac{2 \mid z_1 - z_2 \mid}{d(z_1) + d(z_2)} \tag{5.9}$$

and $a = 1/9$, alternative proposes [8] pp.95, $a = 1/8$.

$b = 2/3$, alternative proposes [8] pp.95, $b = 0.13$.

In the literature there is a disagreement about the values a and b since they have been obtained from measurements on different structures.

Normally, a correlation length λ is defined as

$$\lambda = \int_0^\infty \sqrt{Coh_{C_L}(z_1, z_2, \omega)} \cos(\Phi_{C_L}(z_1, z_2, \omega)) dr \tag{5.10}$$

where r is given by (5.9). λ is typically 1-2.

It should be noticed that the above model is based on a stationary cylinder while measurements were made on a moving cylinder. Therefore the influence of the size of the structure and coherence are ignored, i.e. the lock-in phenomenon is not taken into account.

The model can be used for reinforced concrete structures. However, care should be taken for lightly damped structure such as steel chimneys, [15], [20].

5.2   Motion induced across-wind load

From measurements it is found that lock-in and the correlation is related to the across-wind load due to across-wind vibrations, [2]. The across-wind load per unit length includes an inertia load which is out of phase with the acceleration of the structure, and a negative aerodynamic damping component which is in phase with the velocity of the structure. For most structures this negative damping component $-\zeta_m^{na}$ causes a negative effect on the damping and thereby an increased response.

In Vickery & Basu, [12,13] a negative damping model was proposed which assumes that the vortex shedding induced load has two terms. One term from a stationary cylinder and one term from vortex shedding at a moving cylinder. The motion induced increase in force due to lock-in is then included as an aerodynamic negative damping term. The damping ratio in the across-wind direction for the mth eigen mode is hereby given as

$$\zeta_m = \zeta_m^s + \zeta_m^a - \zeta_m^{na} \tag{5.11}$$

By a modal analysis the response in the across-wind direction can be written

$$y(z, t) = \sum_{m=1}^N q_m(t) \Phi_m(z) \tag{5.12}$$

where q_m : m'th modal coordinate in y-direction.
$\Phi_m(z)$: m'th bending mode shape in y-direction.

The negative aerodynamic damping ratio for the m'th mode shape is assumed to be

$$\zeta_m^{na} = \frac{1}{2\omega_m M_m} \int_0^h c_{na}(z) \Phi_m^2(z) dz \tag{5.13}$$

where M_m is the modal mass for the bending mode shape in the across-wind direction defined by (3.4). The requirement for the negative aerodynamic damping constant c_{na} has to be that the vibration level increases when one of the natural frequencies of the structure controls the vortex shedding frequency, i.e at lock-in ζ_m^{na} is relative large. Further, the response has to be limited, i.e. that ζ_m^{na} has to decrease for increasing vibration level.

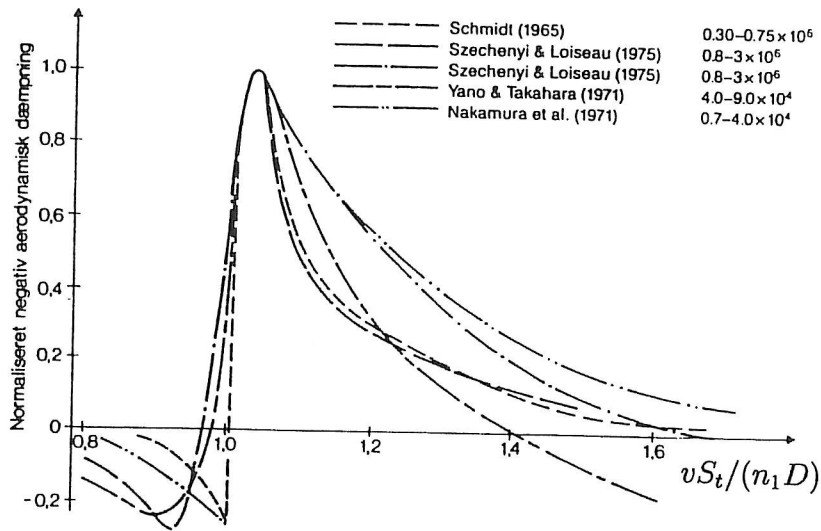In figure 5.1 experimental negative aerodynamic damping results are shown as function of the Reynolds number Re.

Figure 5.1: *Variation of ζ_1^{na} normalized so the maximal value is 1*, [2]

The negative aerodynamic damping constant c_{na} is then proposed to be following non-linear function

$$c_{na}(z) = 2\omega_m \rho d(z)^2 C_{na0}(z) \left(1 - \left(\frac{\sigma_y(z)}{\sigma_{yL}(z)} \right)^\beta \right) \quad (5.14)$$

where C_{na0} is an experimental estimated non-dimensional damping constant for small vibration levels. $\sigma_y(z)$ is the standard deviation of the response as function of the height z obtained from (5.12)

$$\sigma_y^2(z) \approx \sum_{m=1}^{N} \sigma_{qm}^2(t) \Phi_m^2(z) \quad (5.15)$$

assuming well separated natural frequencies.

σ_{yL} is the standard deviation of the limited response, i.e. the maximal response which can be obtained before the vortex shedding will decrease. Therefore, the limiting effect of the response is included in the model by σ_{yL} and the factor β, which is a measure of the decay of ζ_m^{na}. In [12,13] $\beta = 2$ which will be used in the following. The value 1 in

(5.14) corresponds to an assumption of initial maximal negative aerodynamic damping independent of the natural frequency and Re.

It is assumed, that the expression for the standard deviation of the limit response is a linear function of the diameter of the cylinder $d(z)$

$$\alpha = \frac{\sigma_{y_L}(z)}{d(z)} \tag{5.16}$$

From (5.14), (5.15) and substitution of (5.16) into (5.13) it is found that

$$\zeta_m^{na} = A_m - B_m \sigma_{q_m}^2 - \sum_{n=1}^{N} C_{mn} \sigma_{q_n}^2 \tag{5.17}$$

where

$$A_m = \frac{\rho}{M_m} \int_0^h C_{na0}(z) d(z)^2 \Phi_m^2(z) dz \tag{5.18}$$

$$B_m = \frac{\rho}{M_m \alpha^2} \int_0^h C_{na0}(z) \Phi_m^4(z) dz \tag{5.19}$$

$$C_{mn} = \frac{\rho}{M_m \alpha^2} \int_0^h C_{na0}(z) \Phi_m^2(z) \Phi_n^2(z) dz, \quad n \neq m \tag{5.20}$$

By using a white noise approximation the standard deviation of the modal coordinate process follows in the same way as (3.16)

$$\sigma_{q_m}^2 = \frac{S_{P_m^v P_m^v}(\omega_m) + S_{P_m^h P_m^h}(\omega_m)}{8\omega_m^3(\zeta_m^s + \zeta_m^a - \zeta_m^{na}) M_m^2} \tag{5.21}$$

where $S_{P_m^v P_m^v}(\omega_m)$ and $S_{P_m^h P_m^h}(\omega_m)$ are auto-spectra for the modal load for turbulence components and vortex induced components, respectively

$$S_{P_m^v P_m^v}(\omega_m) = \int_0^h \int_0^h \Phi_m(z_1) \Phi_m(z_2) S_{p_y^v p_y^v}(z_1, z_2, \omega_m) dz_1 dz_2 \tag{5.22}$$

$$S_{P_m^h P_m^h}(\omega_m) = \int_0^h \int_0^h \Phi_m(z_1) \Phi_m(z_2) S_{p_y^h p_y^h}(z_1, z_2, \omega_m) dz_1 dz_2 \tag{5.23}$$

$\sigma_{q_m}^2$ is estimated by iteration since $\sigma_{q_m}^2$ is included in the equation for determination ζ_{na}. Normally $\sigma_{q_m}^2$ is analytically estimated from a solution of the second order equation

	$Re < 2 \cdot 10^5$	$2 \cdot 10^5 < Re < 6 \cdot 10^5$	$6 \cdot 10^5 < Re < 3 \cdot 10^6$	$3 \cdot 10^6 < Re$	All
	1	9	37	17	64
σ_{C_L}	–	–	0.17	0.25	0.20
α	1.3	0.8	0.41	0.20	0.70
C_{na0}	2.1	0.6	0.41	0.32	0.30

Table 5.1: *Standard deviation of the lift coefficient σ_{C_L}, α, and C_{na0} as a function of Re* [21].

obtained from (5.21) and (5.17) since it is assumed that only one eigen-mode has to be taken into account. The total variance of the response is given by (5.15).

The parameters σ_{C_L}, α and C_{na0}, relies on experience-based data. In [21] the parameters are estimated from experimental data from 64 chimneys for different values of *Re*. From table 5.1 it is seen that σ_{C_L} approximately is equal to 0.2 for all flow regions. The ratio α between the standard deviation of the limit response and the diameter of the cylinder is in [13] given as 0.4. In [21] a the relationship between *Re* and α is given where α is found to be in the interval [0.2 - 0.4].

5.3 DS 410, Vortex shedding

The following section presents the rules for calculation of the vortex shedding load used in the Danish code for loads on structures (DS410), [1]. These rules are based on a stochastic response model.

The characteristic vortex shedding load per unit length F_w on a structure is given by

$$F_w = m(\omega_1)^2 \Phi_i(z) y_{max} \tag{5.24}$$

where m : mass per unit length.
   ω_1 : 1st eigen-frequency.
   y_{max} : characteristic maximal deflection at the point with largest deflection.
   $\Phi_1(z)$: 1st bending mode shape in y-direction, normalized to 1
      : at the point with largest deflection.

The characteristic maximal deflection at the point with largest deflection y_{max} follows from

$$y_{max} = \sigma_y k_p \tag{5.25}$$

where σ_y : standard deviation of deflection.
   k_p : peak factor.

If it can be assumed that the structure has an uniform distribution of mass, stiffness and

width the standard deviation σ_y can be estimated from

$$\frac{\sigma_y}{b} = \frac{1}{St^2} \frac{C_a}{\sqrt{\zeta_s - K_a \frac{\rho b^2}{m} \left(1 - \left(\frac{\sigma_y}{ba_L}\right)^2\right)}} \frac{\rho b^2}{m} \sqrt{\frac{b}{l}} \tag{5.26}$$

where C_a :   aerodynamic constant.
      K_a :   aerodynamic damping constant.
      a_L :   constant which limits the deflections for light damped structures.
      ζ_s :   structural damping ratio $\delta_s = 2\pi\zeta_s$, see (3.82).
      l :   length or height of structure.

The largest standard deviation σ_y is found for $C_a = C_{a,max}$ given in table 5.2. The standard deviation σ_y can be obtained from

$$\left(\frac{\sigma_y}{b}\right)^2 = c_1 + \sqrt{c_1^2 + c_2} \tag{5.27}$$

where

$$c_1 = \frac{a_L^2}{2}\left(1 - \frac{\zeta_s}{K_a}\frac{m}{\rho b^2}\right)$$

$$c_2 = \frac{a_L^2}{K_a}\frac{\rho b^2}{m}\frac{C_a^2}{St^4}\frac{b}{l} \tag{5.28}$$

For non uniform distribution of mass m and width b the values at the point deflection at the point with largest deflection should be used. If the estimated standard deviation σ_y is smaller than 2 % of the width of the cross section the peak-factor k_p is given by (3.71) where the value of the eigen-frequency is used for ν. If σ_y is larger than 20 % of the cross-section diameter the peak-factor is equal to $\sqrt{2}$. Between these two values the peak-factor is assumed to vary linearly.

The aerodynamic damping constant K_a is given by

$$K_a(I_u) = K_{a,max}h(I_u) \tag{5.29}$$

where $K_{a,max}$ is given in table 5.2. Values of the function h follows from $h(I_u) = 1 - 3I_u$ for $0 \leq I_u \leq 0.25$ and $h(I_u) = 0.25$ for $I_u > 0.25$. The turbulence intensity I_u should be estimated at the point with largest deflection.

For a circular cylinder and for a quadratic section the constants $C_{a,max}$, $K_{a,max}$ and a_L are given in table 5.2. For Reynolds numbers between 10^5 and 10^6 a linear variation of the constants are assumed as a function of the logarithm to the Reynolds number.

It should be noticed that [1] also has simplified rules for calculation of the fatigue load due to vortex shedding if the characteristic vortex shedding load is less than 10 % of the width of the cross section.

constant	circular cylinder $Re \leq 10^5$	circular cylinder $Re = 5 \cdot 10^5$	circular cylinder $Re \geq 10^6$	quadratic section -
$C_{a,max}$	0.02	0.005	0.01	0.04
$K_{a,max}$	2	0.5	1	6
a_L	0.4	0.4	0.4	0.4

Table 5.2: *Constants to be used for vortex shedding calculations.*

5.4   Referencer

1. Danish Standards Association: *Code of Practice for Loads for the Design of Structures* DS 410, 4. edition, 1998.

2. Dyrbye, C. & Hansen, S.O.:, *Wind Loads on Structures*. John Wiley & Sons, 1997.

3. Harris, R.I.: *The Nature of the Wind*. Seminar on Modern Design of Wind-Sensitive Structures, 1970. CIRIA, 1971, p. 29-55.

4. Van Oosterhout, G.P.C.: *The Wind-Induced Dynamic Response of Tall Buildings, a Comparative Study*. J. of Wind Engineering, Vol. 64, 1996, pp. 135-144.

5. Højstrup, J., Larsen, S.E. & Madsen, P.H.: *Power Spectra of Horizontal Wind Components in the Neutral Atmospheric Surface Boundary Layer*. Proceedings of the Ninth Symposium on Turbulence and Diffusion, Risø, 1990, pp. 305-308.

6. Davenport, A.G.: *Gust Loading Factors*. J. of Struc. Div., ASCE, Vol. 93, No. ST3, Juni 1967, p. 11-34.

7. Simiu, E.: *Wind Spectra and Dynamic Alongwind Response*. J. Struc. Div., ASCE, Vol. 100, No. ST9, September 1974, p.1897-1910.

8. Hansen, S.O.: *Vindbelastede skorstene*. Licentiatprojekt fra Afdelingen for Brende Konstruktioner, Danmarks Tekniske Hjskole, Lyngby 1979.

9. Hjort, U.S, & Jensen, M.G.: *Formoptimering af svingningsflsom stlskorsten*, Afgangsprojekt fra K-linien, Aalborg Universitetscenter, 1991.

10. Shiotani, M. & Iwatani, Y.: *Correlations of Wind Velocities in Relation to the Gust Loadings*. Proc. of the III Conf. on Wind Effects on Buildings and Structures, Tokyo, Japan, 1971, p. 57-68.

11. Nielsen, S.R.K.: *Vibration Theory, Vol 1: Linear Vibration Theory*. Aalborg tekniske Universitetsforlag, 1998.

12. Vickery, B.J. & Basu, R.I.: *Across-Wind Vibration of Structures of Circular Cross-Section*, Part I, J. of Wind Engng. and Industrial Aerodyn., Vol 12., No. 1, June 1983.

13. Vickery, B.J. & Basu, R.I.: *Across-Wind Vibration of Structures of Circular Cross-Section*, Part II, J. of Wind Engng. and Industrial Aerodyn., Vol. 12, No. 1, June 1983.

14. Blevins, R.D.: *Flow-Induced Vibration*, Van Nostrand Reinhold Company, New York 1977.

15. Fabricius, C. & Therkelsen F.: *Bestemmelse af en stlskorstens hvirvelinducerede svingninger.* Afgangsprojekt fra K-linien, Aalborg Universitetscenter, 1982.

16. Sigbjrnsson, R.: *On the Theory of Structural Vibrations due to Natural Wind.* Afdelingen for Brende Konstruktioner, Danmarks Tekniske Hjskole, Lyngby, 1974, Rapport R59.

17. Vickery, B.J.: *Progress and Problems in the Prediction of the Response of Prototype Structures to Vortex-Induced Excitation.* J. of Wind Engng. and Industrial Aerodyn., Vol. 33, 1990, p. 181-196.

18. Sarpkaya, T.: *Vortex Induced Oscillations, A Selective Review.* J. of Appl. Mech., Vol. 46, June 1979, p. 241-258.

19. ESDU *Across-Flow Response due to Vortex Shedding.* Nr. 78006, November 1980.

20. Vickery, B.J. & Clark, A.V.: *Lift or Across-Wind Response of Tapered Stacks*, J. of Struc. Div, Vol. 98., No. St1, p. 1-19, 1972

21. CICIND Report, Vol. 2., No. 1, 1986.

22. Nielsen, S.R.K.: *Vibration Theory: Linear Vibration Theory.* Aalborg tekniske Universitetsforlag, July 1998.

23. Clough, W. & Penzien, J.: *Dynamics of Structures.* McGraw-Hill Book Company, Singapore 1982.